



UPPSALA  
UNIVERSITET

*Digital Comprehensive Summaries of Uppsala Dissertations  
from the Faculty of Science and Technology 1772*

# Moisture-Induced Strains and Stresses in Wood

SABINA HUČ



ACTA  
UNIVERSITATIS  
UPSALIENSIS  
UPPSALA  
2019

ISSN 1651-6214  
ISBN 978-91-513-0569-1  
urn:nbn:se:uu:diva-375148

Dissertation presented at Uppsala University to be publicly examined in Högssalen Å10132, Ångströmlaboratoriet, Lägerhyddsvägen 1, Uppsala, Friday, 22 March 2019 at 09:00 for the degree of Doctor of Philosophy. The examination will be conducted in English. Faculty examiner: Sigurdur Ormarsson (Linnaeus University, Faculty of Technology, Department of Building Technology).

### **Abstract**

Huč, S. 2019. Moisture-Induced Strains and Stresses in Wood. *Digital Comprehensive Summaries of Uppsala Dissertations from the Faculty of Science and Technology 1772*. 51 pp. Uppsala: Acta Universitatis Upsaliensis. ISBN 978-91-513-0569-1.

To design safe, reliable and durable timber structures subjected to varying natural outdoor or indoor climates, understanding the long-term behavior of wood when mechanically loaded or restrained to deform is crucial. The present thesis focuses on the numerical modeling of the long-term mechanical behavior of wood. The numerical analysis is divided in the moisture transport and the mechanical analyses. In the moisture analysis, the multi-Fickian moisture transport model is used to determine spatial and temporal moisture content fields over the analyzed domain due to changing relative humidity (*RH*) of the ambient air. The obtained moisture contents are taken into the mechanical analysis where a new mechanical model is applied for predicting rheological response of wood in three orthotropic directions simultaneously. Experimental results of different authors are used to support numerous numerical analyses performed for various wood species, deformation and loading modes in constant or changing *RH* conditions. The performed analyses show that the new mechanical model adequately predicts the viscoelastic behavior of hardwood and softwood species in two orthotropic directions simultaneously under a sustained load or deformation. A significant influence of grain orientation in relation to the applied mechanical load on the viscoelastic creep behavior of wood is observed. The mechanical model is also able to predict accurately the rheological behavior of hardwood subjected to a sustained compressive mechanical load and changing moisture content. Applying the moisture and the mechanical models to the glued-laminated timber specimens during wetting and drying shows good agreement with the experimental results. The magnitudes of moisture-induced stresses perpendicular to the grain indicate a possibility of crack initiation during drying. The influence of characteristic material parameters required in the models on the mechanical state of the analyzed specimens is also determined. A quantification of the viscoelastic and the mechanosorptive material parameters required in the mechanical model is the additional outcome of the performed numerical analyses. The mechanical model presented in this thesis in combination with the multi-Fickian moisture transport model enables a full two- or three-dimensional long-term mechanical analysis of timber members exposed to natural climate with *RH* variations.

*Keywords:* mechanosorption, multi-Fickian moisture transport model, orthotropy, rheology, three-dimensional mechanical model, viscoelasticity, wood

*Sabina Huč, Department of Engineering Sciences, Applied Mechanics, 516, Uppsala University, SE-751 20 Uppsala, Sweden.*

© Sabina Huč 2019

ISSN 1651-6214

ISBN 978-91-513-0569-1

urn:nbn:se:uu:diva-375148 (<http://urn.kb.se/resolve?urn=urn:nbn:se:uu:diva-375148>)

# List of Papers

This thesis is based on the following papers, which are referred to in the text by their Roman numerals.

- I Huč, S., Svensson, S. (2018) Coupled two-dimensional modeling of viscoelastic creep of wood. *Wood Science and Technology*, 52(1):29-43
- II Huč, S., Hozjan, T., Svensson, S. (2018) Rheological behavior of wood in stress relaxation under compression. *Wood Science and Technology*, 52(3):793-808.
- III Huč, S., Svensson, S. (2018) Influence of grain direction on the time-dependent behavior of wood analyzed by a 3D rheological model. A mathematical consideration. *Holzforschung*, 72(10):889-897.
- IV Huč, S., Svensson, S., Hozjan, T. (2018) Hygro-mechanical analysis of wood subjected to constant mechanical load and varying relative humidity. *Holzforschung*, 72(10):863-870.
- V Huč, S., Svensson, S., Hozjan, T. (2018) Numerical analysis of moisture-induced strains and stresses in glued-laminated timber. (*submitted*)

Reprints were made with permission from the respective publishers.

In addition, the work of this thesis was also presented on the following occasions:

- I Huč, S., Hozjan, T., Svensson, S. (2017) Influence of misalignment between direction of observation and wood material orthotropy on viscoelastic strain measurements. CompWood 2017: Computational methods on wood mechanics – from material properties to timber structures, Vienna.
- II Huč, S., Svensson, S. (2017) Coupled two-dimensional modeling of long-term behavior of wood subjected to mechanical stress and varying climatic conditions. CompWood 2017: Computational methods on wood mechanics – from material properties to timber structures, Vienna.
- III Huč, S., Planinc, I., Hozjan, T. (2017) Buckling behavior of timber columns exposed to varying humidity. 3rd International Conference on Multiscale Computational Methods for Solids and Fluids, Ljubljana.
- IV Huč, S., Svensson, S., Hozjan, T. (2018) Numerical modeling of timber structures under varying humidity conditions. Conference proceedings: International scholarly and scientific research & Innovation, Sydney.
- V Hozjan, T., Svensson, S., Pečenko, R., Huč, S. (2018) Rheological behavior of European beech (*Fagus sylvatica*). Engineering Mechanics Institute Conference, Cambridge.
- VI Huč, S., Svensson, S. (2018) Moisture induced stresses and strains in timber members. Engineering Mechanics Institute Conference, Cambridge.

# Contents

1 Introduction.....	7
1.1 Long-term behavior of wood .....	7
1.2 Aims of the thesis .....	8
2 Moisture content in wood .....	10
2.1 Background.....	10
2.2 Moisture transport models .....	11
2.2.1 Multi-Fickian moisture transport model .....	11
3 Rheological behavior of wood .....	15
3.1 Background.....	15
3.1.1 Time-dependent behavior .....	15
3.1.2 Shrinkage and swelling.....	16
3.1.3 Mechanosorptive behavior.....	16
3.2 Rheological models.....	17
3.2.1 Viscoelastic models .....	18
3.2.2 Mechanosorptive models .....	20
3.2.3 Combined models .....	22
3.2.4 New 3D mechanical model.....	23
3.2.5 Material parameters .....	27
4 Results and discussion .....	29
4.1 Viscoelastic material parameters .....	29
4.2 Mechanosorptive material parameters .....	33
5 Conclusions.....	39
Acknowledgements.....	41
Sammanfattning på svenska (Summary in Swedish) .....	42
Povzetek v slovenščini (Summary in Slovenian).....	44
References.....	47



# 1 Introduction

In the absence of fire, insects and fungi, wood is remarkably resistant material, which prove well preserved, centuries old timber structures still serving their purpose [1]. Wood is often a desirable constructional material in residential, industrial, educational and recreational buildings, as well as in infrastructural facilities, owing to be natural, biological, recyclable and renewable. It is used for load-bearing structural members, window frames, furniture, linings, and numerous other products, such as strand boards, cardboards, products in pulp and paper industry, etc. Wood material or simply wood is responsive to the surrounding environment or climate, which, together with its natural imperfections that appear during growth, e.g, knots, reaction wood or resin pockets, influences its long-term performance severely, most often in an unfavorable manner. To enhance its performance and reduce the impact of its disadvantages in construction and other applications, the behavior of wood is experimentally and numerically studied on different scales in the literature, i.e., macroscopic, microscopic, ultrastructural and molecular levels. Many theories for describing physical and mechanical properties exist on each level. In the present thesis, the long-term mechanical behavior of wood is studied on the macroscopic level. Nowadays, in light of the positive attitude towards the environmental friendly living, the use of wood is strongly encouraged, thus, also the timber structures are gaining on popularity. With that, the demand for an enhanced, optimal and efficient design of the long-term mechanical performance of complex timber structures grows and consequently more research is required.

## 1.1 Long-term behavior of wood

The long-term mechanical performance of wood depends on numerous factors, for instance, material properties, mechanical load or deformation modes, and climate conditions with changing temperature and relative humidity ( $RH$ ) of the ambient air. Changes in temperature and/or moisture content in a piece of wood cause deformations also without mechanical loads. In the production and utilization of timber structural members, window frames, furniture, flooring, etc., keeping the deformation during drying or swelling to a minimum is essential. Reducing distortions of timber, such as bowing, cupping, and cracking, especially during drying in an optimal way in terms of time and quality

has been extensively addressed over the years in order to make wood products suitable for construction purposes. Deformations of wood due to differences in temperature are small when compared to deformations resulting from moisture content changes in normal conditions in which structural wood is usually used (approx. temperature  $< 70^{\circ}\text{C}$ , moisture content  $< 30\%$ ) [2]. Moisture has a great influence on wood properties, such as strength, stiffness, toughness, visible appearance, density, resistance to biological degradation, etc. This thesis studies long-term mechanical behavior of wood when exposed to moisture content changes in isothermal conditions. Wood is considered as an orthotropic material with three normal directions, i.e., longitudinal ( $L$  or  $l$ ), radial ( $R$  or  $r$ ) and tangential ( $T$  or  $t$ ). The longitudinal direction points along the grain. The radial and the tangential directions are also named transverse directions, since they are orthogonal to the grain. Clear, healthy wood without imperfections, knots or reaction wood in sheltered environment, i.e., not directly exposed to weather impacts, such as rain or sun, is considered in the thesis.

## 1.2 Aims of the thesis

The focus of the present thesis, which main body are the enclosed papers, is on the multi-dimensional numerical modeling of the long-term behavior of wood (Papers I - V). The modeling is supported by the experimental results of self-performed tests (Paper II) and tests from the literature (Papers I, IV, V). For that purpose, a new mechanical model, enabling coupled simultaneous response of wood in three orthotropic directions, is implemented in a finite element software for constant environmental conditions (Papers I - III) and changing  $RH$  of the ambient air (Papers IV, V). Spatial and temporal moisture content fields within wood due to changing  $RH$  needed as the input to the mechanical model are determined with an advanced moisture transport model, which is also implemented in the same finite element software. The main aim of the thesis is to investigate the possibilities and accuracy of the new mechanical model to predict the long-term behavior of softwood and hardwood materials under various mechanical excitation modes and climate conditions. In the scope of the thesis, the following studies are performed:

In **paper I**, three variants of the new mechanical model are applied to predict the viscoelastic creep response in two orthotropic directions of four different wood species exposed to a sustained constant tensile or shear load. The required viscoelastic material parameters in each variant of the mechanical model are determined by a fitting procedure of the numerical results to the experimental results from the literature.

**Paper II** experimentally and numerically examines the viscoelastic behavior of softwood in stress relaxation. Tests with the applied stepwise constant uniaxial deformation along and perpendicular to the grain were carried out to evaluate the ability of the three variants of the mechanical model to predict stress relaxation of wood.

**Paper III** is a theoretical paper where the symmetry of the viscoelastic compliance matrix of the mechanical model is mathematically shown. The influence of grain orientation on the time-dependent behavior of wood is numerically analyzed. Small misalignments of the material orthotropic directions relative to the directions of observation and applied tensile load are examined, which is crucial to account for when interpreting the obtained experimental results.

**Paper IV** presents a numerical hygro-mechanical analysis of a wood specimen subjected to a constant compressive mechanical load and varying  $RH$ . The multi-Fickian moisture transport model and the new mechanical model are used in the hygro-mechanical analysis. A set of the viscoelastic and the mechanosorptive material parameters of hardwood is obtained by a fitting procedure between the numerical and the experimental results.

**Paper V** numerically analyzes moisture-induced strains and stresses in glued-laminated timber member during wetting and drying due to changing  $RH$  of the ambient air. The multi-Fickian moisture transport model and the mechanical model coupled in two material directions in the cylindrical coordinate system are applied in the analyses. The influence of characteristic material parameters required in the numerical models on the mechanical behavior of the analyzed timber member and the possibility of crack initiation are also examined.

## 2 Moisture content in wood

### 2.1 Background

Wood is a natural organic open porous material, which exchanges water with the atmosphere. When dry, it takes water from the atmosphere and the opposite, when wet, it gives moisture to the atmosphere. The processes of gaining or losing water progress until an equilibrium moisture content is attained, which is in equilibrium with the water vapor pressure of the atmosphere. The equilibrium moisture content depends on whether the equilibrium is reached from a lower or a higher  $RH$  of the ambient air. The two relationships between the moisture content in wood,  $u$ , and  $RH$  are referred to as the adsorption and the desorption isotherms. Wood exposed to cyclic  $RH$  changes takes the states of  $u$  between the sorption isotherms in a hysteretic form as shown in Figure 1. Theoretical descriptions of the sorption isotherms are based on empirically determined data [3-5] for various wood species and temperatures.

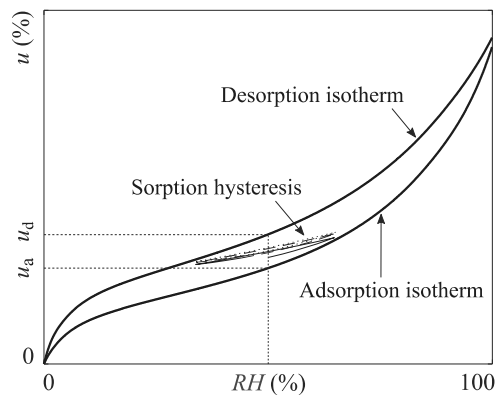


Figure 1. Moisture content in wood,  $u$ , in relation to relative humidity of the ambient air,  $RH$ , at constant temperature.

Water in wood is present as free water in cell lumens, which is in liquid and/or vapor states and as bound water in cell walls. Moisture content is a measure of the amount of water contained in a piece of wood and defined as a ratio of the mass of water in wood to the mass of dry wood. The mass of water in wood is determined as the difference between the total mass of wood and its mass when oven-dried [6]. The values of moisture content greater than 100% are normal for sapwood of freshly cut logs. In freshly cut wood, the cell walls are

water saturated and the cell lumens contain water in liquid or liquid-vapor states. After cutting, a substantial loss of water occurs. Eventually, the cell walls reach unsaturated states. The transition zone from saturated to unsaturated states is defined as a fiber saturation point (FSP). Several definitions of the FSP are reported in the literature, however, in theory, the moisture content of approximately 30% - 40% corresponds to  $RH$  of 100% for wood in equilibrium with the atmosphere [7]. The influence of moisture content on wood properties, such as density, stiffness, and strength, is significant below the FSP, which are the conditions structural wood is normally used in. Thus, in this thesis, the rheological behavior of wood is studied below the FSP.

## 2.2 Moisture transport models

Flow of water below the FSP includes the diffusion of water vapor through the pores and the cell lumens and the diffusion of bound water in the cell walls. Thus, the moisture transport in wood is most often described simply by the Fickian diffusion equation [8-12]

$$\frac{\partial u}{\partial t} = \nabla \cdot (\mathbf{D} \nabla u) \quad (1)$$

where  $\mathbf{D}$  is the diagonal diffusivity tensor. On the boundaries, the moisture flow from the ambient air into wood across the surface,  $q_n$ , is described as

$$\frac{q_n}{\rho_0} = S (u_{air} - u_{surf}) \quad (2)$$

where  $\rho_0$  is the dry density of wood,  $S$  the surface emissivity,  $u_{air}$  the equilibrium moisture content corresponding to  $RH$  of the ambient air and  $u_{surf}$  the moisture content in wood on the macroscopic surface. The sorption hysteresis is not accounted for in Eqs. (1) and (2). Since this simple approach or model does not appropriately describe the moisture transport in wood [13, 14], an advanced and physically feasible moisture transport model, the multi-Fickian model, was developed [15-17]. A recent comparison of both moisture transport models is given in [18]. In this thesis, the multi-Fickian moisture transport model is used to determine spatial and temporal moisture content fields in the analyzed wood specimens.

### 2.2.1 Multi-Fickian moisture transport model

The multi-Fickian moisture transport model adequately describes the complex moisture transport system in wood by accounting for the bound water and the

water vapor diffusion processes, their coupling through sorption, and the hysteresis effect. Thus, more realistic moisture content gradients are predicted within the analyzed specimens, which results in more accurate predictions of moisture-induced strains and stresses due to changing climate conditions. The model's mathematical formulation and the application examples are thoroughly presented in [15-17, 19, 20]. In brief, the pressure formulation of the three-dimensional (3D) multi-Fickian moisture transport model has two governing equations

$$\frac{\partial}{\partial t} \left( p_v \frac{\varphi M}{R_g T_s} \right) = \nabla \cdot \left( \mathbf{D}_v \nabla \left( p_v \frac{\varphi M}{R_g T_s} \right) \right) - \dot{c} \quad (3)$$

$$\frac{\partial c_b}{\partial p_{vw}} \frac{\partial p_{vw}}{\partial t} = \nabla \cdot \left( \mathbf{D}_b \frac{\partial c_b}{\partial p_{vw}} \nabla p_{vw} \right) + \dot{c} \quad (4)$$

where the unknowns are  $p_v$ , the partial vapor pressure in water vapor phase, and  $p_{vw}$ , the imaginary pressure that is related to  $c_b$ , the concentration of water in bound water phase.  $T_s$  denotes the prevailing temperature,  $R_g$  the universal gas constant,  $M$  the molar mass of water,  $\varphi$  the porosity of wood and  $t$  time. The operator,  $\nabla = \left( \frac{\partial}{\partial x}, \frac{\partial}{\partial y}, \frac{\partial}{\partial z} \right)$ , defines that the mathematical formulation of the moisture transport model is expressed in the Cartesian coordinate system  $xyz$ , which may coincide with the material orthotropic directions,  $R$ ,  $T$  and  $L$ . Sorption rate,  $\dot{c}$ , is the connecting term in Eqs. (3) and (4), and presents the driving force for the moisture transport processes to occur

$$\dot{c} = H_p(p_v - p_{vw}) \quad (5)$$

where  $H_p$  is the reaction rate function when  $p_{vw} < p_v$

$$H_p = C_1^p \exp \left( - \left( c_{21}^p \exp(c_{22}^p p_{vw}/p_s) \right) (p_{vw}/p_v)^{c_3^p} \right) + C_4^p \quad (6)$$

and when  $p_{vw} > p_v$

$$H_p = C_1^p \exp \left( - \left( c_{21}^p \exp(c_{22}^p p_{vw}/p_s) \right) (2 - p_{vw}/p_v)^{c_3^p} \right) + C_4^p. \quad (7)$$

The constants,  $C_1^p$ ,  $c_{21}^p$ ,  $c_{22}^p$ ,  $c_3^p$ , and  $C_4^p$ , are empirically determined.  $p_s$  is the saturated vapor pressure of the ambient air at  $T_s$ . The inequalities  $p_{vw} < p_v$  and  $p_{vw} > p_v$  denote the uptake (adsorption) and the loss (desorption) of water vapor in wood, respectively. The empirical expressions (8) [21] and (9) [22] estimate the diffusivity of water vapor in the cell lumens and the diffusivity of bound water in the cell walls, respectively,

$$\mathbf{D}_v = \begin{bmatrix} \xi_x & 0 & 0 \\ 0 & \xi_y & 0 \\ 0 & 0 & \xi_z \end{bmatrix} \left( 2.31 \cdot 10^{-5} \frac{p_{atm}}{p_{atm} + p_v} \left( \frac{T_s}{273} \right)^{1.81} \right) \quad (8)$$

$$\mathbf{D}_b = \begin{bmatrix} D_{x,0} & 0 & 0 \\ 0 & D_{y,0} & 0 \\ 0 & 0 & D_{z,0} \end{bmatrix} \exp \left( - \frac{10^3 (38.5 - 29u)}{R_g T_s} \right) \quad (9)$$

where  $p_{atm}$  is the atmospheric pressure,  $\xi_x$ ,  $\xi_y$ , and  $\xi_z$  are the flow resistances by the material's internal pore structure in  $x$ ,  $y$ , and  $z$  directions, respectively.  $D_{x,0}$ ,  $D_{y,0}$  and  $D_{z,0}$  are the diffusivity coefficients in the material directions  $x$ ,  $y$ , and  $z$ , respectively. The concentration of water in bound water phase,  $c_b$ , is related to the moisture content as

$$c_b = \rho_0 u. \quad (10)$$

The moisture content in wood is determined as

$$u = s (u_d - u_a) + u_a \quad (11)$$

where the adsorption ( $i = a$ ) and desorption ( $i = d$ ) isotherms are defined as in [23]

$$u_i = \frac{p_{vw}/p_s}{k_i^1 + k_i^2 p_{vw}/p_s + k_i^3 (p_{vw}/p_s)^2}. \quad (12)$$

The material parameters,  $k_i^1$ ,  $k_i^2$  and  $k_i^3$ , are adsorption ( $i = a$ ) and desorption ( $i = d$ ) coefficients that can be empirically determined. The sorption hysteresis is modelled by the following so-called scanning curves

$$s = \begin{cases} -1 + 2E_1^a E_2^a & \dot{p}_{vw} > 0 \wedge s_0 > 0 \\ 0 & \dot{p}_{vw} > 0 \wedge s_0 = 0 \\ 2 - 2E_1^d E_2^d & \dot{p}_{vw} < 0 \wedge s_0 < 1 \\ 1 & \dot{p}_{vw} < 0 \wedge s_0 = 1 \end{cases} \quad (13)$$

where

$$E_1^a = (1 - p_{vw}/p_s) / (d_2^{q_2} (1 - p_{vw,0}/p_s)^{(1+q_2)}), \quad (14)$$

$$E_2^a = d_1 / \ln \left( \left( d_2 (1 - p_{vw,0} / p_s) \right)^{(1+q_2)} \right), \quad (15)$$

$$E_1^d = (p_{vw} / p_s) / \left( d_2^{q_1} (p_{vw,0} / p_s)^{(1+q_1)} \right), \quad (16)$$

$$E_2^d = d_1 / \ln \left( \left( d_2 p_{vw,0} / p_s \right)^{(1+q_1)} \right), \quad (17)$$

$$q_1 = - \frac{\ln(\ln(2)) - \ln(\ln(2-s_0))}{\ln(\ln(2)) - \ln(\ln(2-s_0)) - d_1'} \quad (18)$$

$$q_2 = - \frac{\ln(\ln(2)) - \ln(\ln(1+s_0))}{\ln(\ln(2)) - \ln(\ln(1+s_0)) - d_1}. \quad (19)$$

$p_{vw,0}$  and  $s_0$  are the values of  $p_{vw}$  and  $s$  at the previous time step, respectively, and  $d_1$  and  $d_2$  are the shape parameters.

To solve the differential equations (3) and (4), the partial vapor pressure at the specimen's macroscopic surface,  $p_v^s$ , is assumed to be equal to the partial vapor pressure of the ambient air,  $p_v^a = RH p_s$ ,

$$p_v^s = p_v^a. \quad (20)$$

Eq. (21) states that the bound water, which presence is restricted to solid wood material, cannot pass through the surface

$$\mathbf{n} \cdot \mathbf{J}_b = 0 \quad (21)$$

where  $\mathbf{n}$  is the normal vector to the surface and  $\mathbf{J}_b$  is the flux vector of bound water.

## 3 Rheological behavior of wood

### 3.1 Background

#### 3.1.1 Time-dependent behavior

The mechanical response of wood subjected to a sustained load or deformation is not constant over time, and thus characterized as time-dependent. The magnitude of the time-dependent response is influenced by many factors, i.e., the magnitude of the mechanical excitation, density and grain orientation. The mechanical behavior of wood is also very much dependent on the moisture state and temperature. Commonly, wood exhibits the time-dependent behavior also known as viscoelastic behavior in constant climate conditions where no moisture content or temperature variations occur. The viscoelastic behavior is associated with two phenomena: 1) creep of deformation, which occurs when the deformations of a wood piece subjected to the sustained mechanical load increase with time, and 2) relaxation of stress, which occurs when the deformation is induced and restrained in a wood piece. Usually, in timber utilization, timber members maintain the mechanical loads. Therefore, much more experimental and numerical research on creep of strain than relaxation of stress in wood has been carried out over the years. In general, at lower levels of applied stress, the rate of deformation decreases with time and the deformation is recoverable when unloaded. At high stress levels, a part of the induced deformation does not recover, thus it is permanent or plastic. In such cases, the rate of deformation, after initial rapid increase (primary creep), is almost constant during an intermediate period (secondary creep), followed by another rapid increase leading towards failure (tertiary creep) as illustrated in Figure 2. During the period of primary creep, it is expected for wood to behave in accordance with the principles of solid mechanics and the theory of linear viscoelasticity. A typical or normal behavior of wood during primary creep is characterized when, for instance, the applied sustained tensile uniaxial mechanical load in one of the orthotropic directions causes extending in that direction and contracting of the material in the other two orthotropic directions. Likewise, the sustained compressive mechanical load in one of the material's orthotropic directions causes contracting in that direction and extending of the material in the other two orthotropic directions. Naturally, the influence of grain orientation relative to the orientation of mechanical excitations on the

time-dependent behavior of wood is expected, which needs to be addressed and quantified properly to interpret the observed wood behavior correctly.

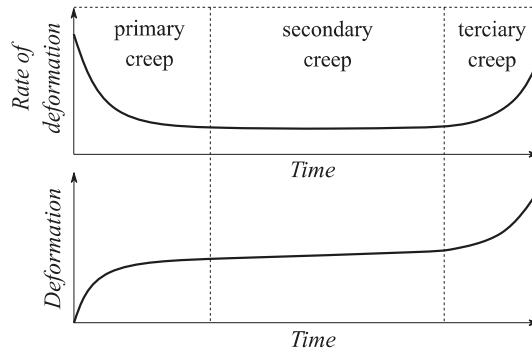


Figure 2. A schematic illustration of the deformation and the rate of deformation over time in a piece of wood subjected to a sustained constant load.

### 3.1.2 Shrinkage and swelling

Shrinkage and swelling are a reduction and an increase of dimensions, respectively, caused by moisture content changes in a piece of wood. In the literature, hygroexpansion is a common expression, including both phenomena. The substantial dimensional changes in wood occur first after cutting a tree when the reduction of moisture content is present while the material dries. Though smaller in magnitude, the dimensional changes also occur due to changes of  $RH$  of the ambient air. Fairly small variations of  $RH$  in natural climate occur on daily basis, while the  $RH$  variations on yearly basis are higher in the climate zones typical for Europe. Since the diffusion of water vapor in a piece of wood is a slow process, a considerable delay is present between the piece's inner and outer parts. A non-uniform distribution of moisture content in a wood piece results in moisture gradients, which constrain shrinkage and swelling strains in the piece. Due to the anisotropic nature of wood, the degree of shrinkage and swelling is different in the three normal directions. The variation in the shrinkage and swelling behavior is also present among the different wood species. In general, the tangential shrinkage is approximately twice as the radial, while the ratio between the longitudinal shrinkage and the shrinkage in the transverse directions is about 1:40 [2, 6].

### 3.1.3 Mechanosorptive behavior

Moisture content changes and mechanical loads, acting simultaneously, cause additional increase in deformations of wood. This acceleration of creep with variable moisture content was already reported in early 1960s [24-26]. Grossman [27] used the term mechano-sorptive effect for an increased deflection of

a loaded beam exposed to moisture cycling in comparison with immediate deflection caused by a constant load. Since then, the terms mechanosorptive behavior, response, strain or shortly mechanosorption are most commonly found in the literature to describe the response of wood material caused by the simultaneous interaction of the moisture content change and the mechanical loading or restraint. Since the moisture content changes cause shrinkage or swelling and the mechanical loads the time-dependent creep, the mechanosorption can never occur by itself. To quantify the three characteristic rheological behaviors of wood, multiple experiments are usually carried out on different material scales. The obtained experimental results are used to calibrate the mathematical models for predicting the rheological behavior of wood. Over the years, different theories were applied in an attempt to model each phenomenon separately and combined. The mathematical formulations started in one dimension, which with the development of computers eventually improved to two and three dimensions. Nevertheless, the long-term behavior of wood has been studied for decades, it still seems not to be fully understood. The possibilities of its accurate numerical predictions are quite limited as well.

### 3.2 Rheological models

Although the time-dependent behavior, the shrinkage and swelling, and the mechanosorptive behavior of wood cannot be adequately separated, the superposition principle of strains is commonly used as a general assumption in mathematical models. For one-dimensional (1D) case the assumption is written as

$$\varepsilon = \varepsilon^e + \varepsilon^{ve} + \varepsilon^s + \varepsilon^{ms} \quad (22)$$

where the total strain,  $\varepsilon$ , comprises of the following contributions: the elastic strain,  $\varepsilon^e$ , the viscoelastic strain,  $\varepsilon^{ve}$ , the shrinkage or swelling strain,  $\varepsilon^s$ , and the mechanosorptive strain,  $\varepsilon^{ms}$ . The assumption in Eq. (22) occasionally takes the rate form

$$\dot{\varepsilon} = \dot{\varepsilon}^e + \dot{\varepsilon}^{ve} + \dot{\varepsilon}^s + \dot{\varepsilon}^{ms} \quad (23)$$

where a dot (.) designates the time derivative. Each strain contribution is normally modelled with an individual mathematical expression. The most common mathematical expression for modeling shrinkage and swelling of wood based on empirical results is a linear relation between the shrinkage and swelling strain, and the difference between the reference and the current moisture contents. Since the behavior of wood is in general time-dependent, it can never be truly elastic. Nevertheless, an acceptable simplification is adopted that the

behavior of wood at low stress or strain levels and short periods of time is treated as elastic. The elastic response is associated with the recoverable part of deformation after unloading and modelled by Hooke's law [28]. The limit of transition from almost linear to highly nonlinear behavior of wood varies with the mode of testing, wood species, environmental conditions, etc. At constant  $RH$  and temperature, it was found that 50% of the ultimate stress is an approximate limit of the linear viscoelastic behavior of wood under compression, bending and tension [2]. In most practical applications, working stresses are rarely exceeding 50% of the ultimate stress; therefore, it is reasonable to assume that wood behaves as the linear viscoelastic material under normal service conditions [2].

### 3.2.1 Viscoelastic models

The theory of linear viscoelasticity [29-31], which was developed in the analogy to the theory of linear elasticity, showed to be very useful for describing the long-term mechanical behavior of wood. The conventional 1D viscoelastic models consist of the elements called a spring and a dashpot. The spring represents the linear elastic behavior of the material, written mathematically as (Hooke's law)

$$\sigma = E \varepsilon^e \quad (24)$$

where  $\sigma$  is the stress and  $E$  the elastic modulus. The viscous behavior of the material is characterized by the linear dashpot with the constitutive relation

$$\sigma = \eta \dot{\varepsilon}^v \quad (25)$$

where  $\eta$  is the dashpot viscosity and  $\dot{\varepsilon}^v$  the rate of viscous strain. The simplest rheological models are combinations of the spring and the dashpot in series, i.e., the Maxwell model in Figure 3a, or in parallel, i.e., the Kelvin-Voigt model or simply the Kelvin model in Figure 3b [30]. The differential equations of the Maxwell model or unit and the Kelvin model or unit are written as

$$\dot{\sigma}/E + \sigma/\eta = \dot{\varepsilon}^{ve} \quad (26)$$

and

$$\sigma = E \varepsilon^{ve} + \eta \dot{\varepsilon}^{ve}, \quad (27)$$

respectively, where  $\dot{\sigma}$  is the stress rate and  $\dot{\varepsilon}^{ve}$  the rate of viscoelastic strain. The viscoelastic strain,  $\varepsilon^{ve}$ , is the sum of the elastic and the viscous strains in Eq. (26),  $\varepsilon^{ve} = \varepsilon^e + \varepsilon^v$ , while it equals the elastic and the viscous strains in Eq. (27),  $\varepsilon^{ve} = \varepsilon^e = \varepsilon^v$ .

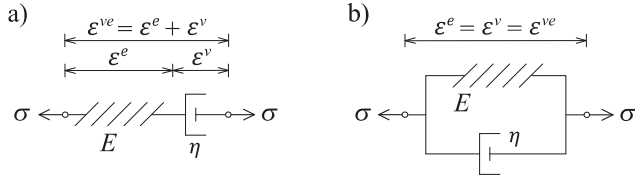


Figure 3. Simple rheological models a) Maxwell and b) Kelvin units.

In the viscoelastic constitutive equations, the creep compliance and the relaxation modulus are defined as the connecting terms between  $\sigma$  and  $\varepsilon^{ve}$  [29, 31]. For example, the creep compliance of the Maxwell model is defined as the creep strain per unit of applied constant stress and determined as

$$J(t) = 1/E + 1/\eta t. \quad (28)$$

The relaxation modulus of the Maxwell model determined as

$$R(t) = E \exp(-E t/\eta) \quad (29)$$

is defined as the stress per unit of applied constant strain. Obviously, the creep compliance and the relaxation modulus are not constants and their relation is not inversely proportional. The relaxation modulus and the creep compliance are recognized as the time-dependent material properties, thus, the latter is often used to present the viscoelastic response of wood in the literature [32-37]. The more complex viscoelastic models consist of numerous springs and dashpots and combinations of the Maxwell and the Kelvin units.

The constitutive equations of the viscoelastic models can also be described by means of the hereditary integrals. Since wood is usually considered as an orthotropic material in mathematical formulations, the hereditary integral representation of the viscoelastic constitutive equations is generalized to three dimensions [28, 29, 38] as follows

$$\varepsilon_{ij}(t) = \int_0^t J_{ijkl}(t - \tau) \frac{\partial \sigma_{kl}}{\partial \tau} d\tau \quad (30)$$

$$\sigma_{ij}(t) = \int_0^t C_{ijkl}(t - \tau) \frac{\partial \varepsilon_{kl}}{\partial \tau} d\tau \quad (31)$$

where  $\tau$  is the time or integration variable,  $\varepsilon_{ij}$  and  $\sigma_{ij}$  are the components of the strain and the stress tensors, respectively,  $J_{ijkl}$  is the component of the fourth order creep compliance tensor and  $C_{ijkl}$  is the component of the fourth order relaxation tensor. In Eqs. (30) and (31), the principle of Boltzmann's superposition is used. For Eq. (30), the principle of Boltzmann's superposition

states that the separate creep strain responses to two constant stresses applied at two consecutive times give, if summed, the same creep strain response as if the same two constant stresses are acting together as a sum. Considering the interchange of the stresses and the strains holds for Eq. (31).

In the literature, various mathematical formulations of the 3D viscoelastic compliance matrix are found. Theoretically, the viscoelastic compliance matrix has to be symmetric [29, 39, 40], which is fulfilled seldom, since only a few formulations of the symmetric viscoelastic matrices are found in the literature [12, 41]. Quite frequently, formulations of the viscoelastic compliance matrix include time-dependent Poisson's ratios. In theory [31], the time-dependent Poisson's ratio is directly defined from the measurements of stress relaxation and a conversion is needed if creep strain measurements are used for its determination. Practically, the time-dependent Poisson's ratios are often determined from uniaxial and lateral strain measurements in creep experiments [32, 42-46] analogous to the theory of elasticity without the conversion. Consequently, the components of the viscoelastic compliance matrix, which include the time-dependent Poisson's ratios from creep tests that are determined in a theoretically inconsistent manner, cannot return the symmetry of the viscoelastic compliance matrix. The mathematical definitions and the existence of the time-dependent Poisson's ratios in linear viscoelasticity are further discussed in [47-49]. Additionally, Frandsen [49] showed that scaling of the off-diagonal components to the diagonal components of the viscoelastic or the elastic compliance matrices is not straightforward when accounting for the symmetry of the viscoelastic compliance matrix and the time-dependence of the Poisson's ratios.

### 3.2.2 Mechanosorptive models

Once established that moisture influences the mechanical behavior of wood severely, the mathematical formulations of mechanosorption emerged in analogy to the viscoelastic spring-dashpot type models. The work of Ranta-Maunus [50] is often, among [26, 51, 52], referred to as the most elementary and the first analytical description of mechanosorptive creep in terms of continuum mechanics [27, 53]. The initial 1D integral formulation of a hydroviscoelastic theory to describe creep deformations due to moisture content variations is rearranged in differential form in [54]. The most elementary models or so-called mechanosorptive Maxwell models [53] describe the elastic deformation with a spring, and the development of the mechanosorptive creep with a dashpot where the time differential in the conventional equation of the linear dashpot (Eq. (25)) is replaced by the absolute value of the moisture content change differential  $|du|$ . The corresponding equation, describing the mechanosorptive dashpot, takes the form

$$\frac{d\varepsilon^{ms}}{|du|} = m \sigma \quad (32)$$

where the parameter  $m$  is the inverse of the viscosity of moisture change induced creep. These models do not include recovery creep that is when the load is removed and the moisture content continues to change. More advanced models, namely mechanosorptive Kelvin type models [53] can describe the recoverability of the mechanosorptive creep. In these models introduced in [55-57], the mechanosorptive dashpot is placed in parallel with the spring. The mechanosorptive Kelvin models show to be better in predicting the mechanosorptive behavior of wood than the mechanosorptive Maxwell models. Thus, they are widely used in different forms among various researchers, e.g., [8, 58-63].

David Hunt with coauthors performed extensive experimental and numerical studies of the mechanosorptive creep with special emphasis on examining whether the mechanosorptive creep approaches the strain or deformation limit [55, 64-66]. The physical ageing theory [67, 68], which is explained as time-dependent approach to equilibrium, is also considered in attempts to clarify the mechanosorptive behavior of wood material. Another interesting phenomenon that is given much attention is the locking effect, characterized as an increase of strain during the first phases of moistening and blocking of strain during the drying phases [69-71].

The mechanosorptive Kelvin models are used to describe the behavior of wood due to moisture content changes alone and simultaneously with mechanical loads or deformations, as well as to simulate drying stresses in the kiln drying process of timber products. The latter phenomenon is experimentally and numerically studied in [58-60, 72-74] where the mechanosorptive Kelvin model from [75] is modified with a time shift factor that accounts for the temperature and moisture content changes.

In some models [12, 76], the dependence of the elastic and the shear moduli on the moisture content is accounted for, since it is experimentally confirmed that they linearly decrease with the increase of moisture content below the FSP. Further increase in moisture content above the FSP has no influence on the elastic and the shear moduli. The moisture content increase has a larger effect on the elastic moduli perpendicular to the grain than on the modulus along the grain [2, 77] as schematically shown in Figure 4.

3D mechanosorptive models are formulated in a similar fashion than the 3D viscoelastic models where the components of the mechanosorptive compliance matrix are usually scaled to the components of the linear elastic compliance matrix. Hanhijärvi and Mackenzie-Helnwein [78] formulated a 3D mechanical model of wood in changing environmental conditions by means of the thermodynamic principle. A partially irrecoverable mechanosorptive

creep deformation is described by the use of a theory of plasticity with a combination of isotropic and kinematic hardenings. The obtained set of partial differential equations was solved with a numerical time integration algorithm shown in [79]. The proposed 3D thermodynamic formulation for modeling the long-term behavior of wood [78] is applied in several studies [8, 9, 80].

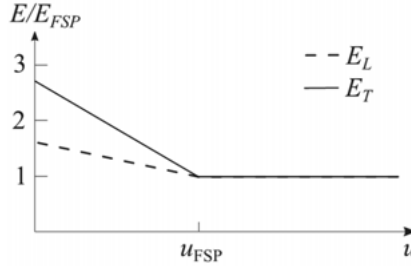


Figure 4. A schematic representation of the influence of the moisture content,  $u$ , on the elastic moduli along,  $E_L$ , and perpendicular,  $E_T$ , to the grain normalized against the magnitude of the moduli at the fiber saturation point, FSP, at room temperature.

### 3.2.3 Combined models

After several years of analyzing wood experimentally in different manners, it was proposed that the mechanosorptive and the viscoelastic behaviors, as well as creep and relaxation, are connected in a way that trigger the same molecular mechanisms of breaking and remaking of hydrogen bonds when subjected to the mechanical excitation and the changing moisture content [14, 67, 81-85]. Thus, the mathematical approach with separating the phenomena (Eq. (22)) needs to be appropriately modified when applying the spring-dashpot type models. A simple 1D combined spring-dashpot model could include the spring placed in parallel with the series of the viscoelastic Maxwell unit and the mechanosorptive dashpot as suggested in [53]. Another approach assuming the mechanosorptive creep and the viscoelastic creep correlation, based on the theory of molecular deformation kinetics is found in the literature [82, 84, 86-89]. In the theory of molecular deformation kinetics, a nonlinear 1D flow equation is derived [90]. The theory is adapted for modeling the creep behavior of wood where flow is associated with breaking and remaking of hydrogen bonds. The 1D constitutive equation of a nonlinear dashpot is written as

$$\dot{\varepsilon}^{ve} = A \sinh(B \sigma), \quad (33)$$

describing the viscoelastic behavior where  $A$  and  $B$  are the state-dependent material parameters. In [82], Eq. (33) is modified to include also the mechanosorptive creep. The given nonlinear expression is then summed with the equations of linear elastic spring and the shrinkage and swelling unit, all together forming one rheological assembly. Ten of these rheological assemblies

are put in parallel to form the full model. The 1D rheological models for wood formulated on the theory of deformation kinetics captured the experimental results quite good in general. Therefore, their extrapolation to three dimensions seems a natural next step, however, to the author's best knowledge, the theory of deformation kinetics applied in three dimensions has not been presented yet in the literature.

### 3.2.4 New 3D mechanical model

In this thesis, a new 3D mechanical model is applied to analyze the rheological behavior of wood. Its formulation is based on Frandsen's [49] two-dimensional (2D) viscoelastic model of the spring-dashpot type. The new 3D mechanical model is able to simulate a response of an orthotropic material in three orthotropic directions simultaneously when exposed to  $RH$  changes and mechanical excitations in one or more directions. Each normal material direction consists of the same rheological assembly of the spring, two Kelvin units, and the shrinkage and swelling unit in series. The springs return the elastic responses, and the Kelvin units the viscoelastic and the mechanosorptive responses. Figure 5 illustrates the new 3D mechanical model in normal directions where the stress excitation  $\sigma_i$  is applied. Indexes  $i$ ,  $j$ , and  $k$  run for the material orthotropic directions  $x$ ,  $y$ , and  $z$ , which can naturally be replaced with the orthotropic directions of wood, i.e.,  $R$ ,  $T$  and  $L$ . Indexes  $i$ ,  $j$ , and  $k$  never represent the same material direction that yields six possible combinations (i.e.,  $i = x, j = y, k = z$ ;  $i = x, j = z, k = y$ ;  $i = y, j = x, k = z$ ; etc.). The summation convention for indexes  $i$ ,  $j$ , and  $k$  does not apply.

Since the shear behavior of the orthotropic material is independent of the mechanical behavior in normal directions, it is represented by the 1D spring-dashpot model as depicted in Figure 6. Indexes  $\alpha\beta$  stand for the shear planes  $xy$ ,  $yz$  and  $zx$ . Subscripts of the material parameters associated with shear include the suffix  $s$ .

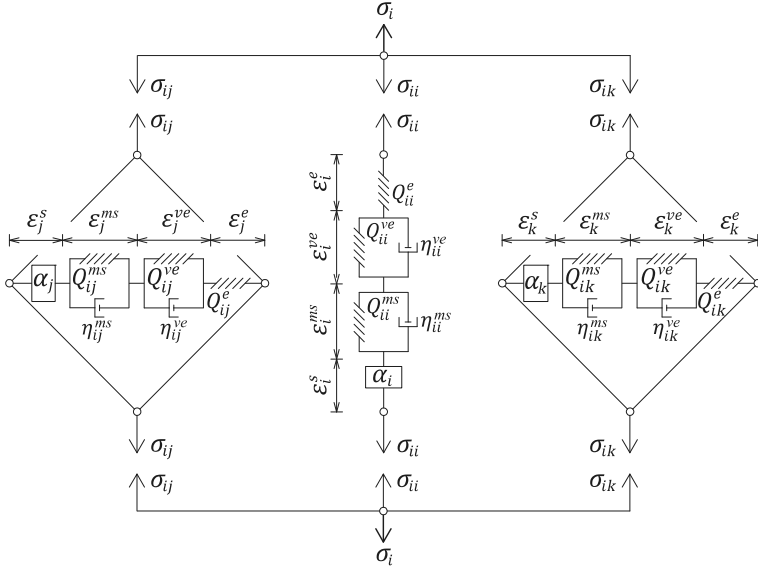


Figure 5. An illustration of the new 3D mechanical model for the orthotropic directions  $i$ ,  $j$ , and  $k$  when the stress excitation  $\sigma_i$  is applied. The corresponding response is expressed in terms of strains in the direction of excitation,  $\epsilon_i$ , and the two perpendicular directions,  $\epsilon_j$  and  $\epsilon_k$ . The elastic, the viscoelastic, the mechanosorptive and the shrinkage and swelling contributions are designated by  $e$ ,  $ve$ ,  $ms$  and  $s$ , respectively. The spring stiffnesses are designated by  $Q$ , the dashpot viscosities by  $\eta$  and the shrinkage and swelling coefficients by  $\alpha$ .

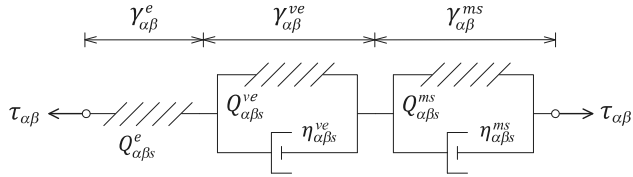


Figure 6. An illustration of the mechanical model for the shear plane  $\alpha\beta$ .  $\tau_{\alpha\beta}$  is the shear stress,  $\gamma_{\alpha\beta}^e$  the elastic,  $\gamma_{\alpha\beta}^{ve}$  the viscoelastic and  $\gamma_{\alpha\beta}^{ms}$  the mechanosorptive shear strain.  $Q$ 's and  $\eta$ 's are the material parameters that specify the spring stiffnesses and the dashpot viscosities, respectively.

A mathematical formulation of the new 3D spring-dashpot mechanical model is based on the same stress-strain decomposition principle as it is applied in the derivation of differential equations of 1D spring-dashpot rheological models (section 3.2.1). The constitutive equations in normal directions of the new 3D mechanical model are derived by considering the model's graphical representation in Figure 5 where only one stress excitation in normal direction,  $\sigma_i$ , is applied at a time. The full constitutive description of the mechanical model in normal directions when the excitations are applied in multiple directions is obtained by interchanging the indexes,  $i$ ,  $j$ ,  $k$ , and their association

with the material orthotropic directions,  $x, y, z$ . Once applied,  $\sigma_i$  is immediately decomposed along the three orthotropic material directions

$$\sigma_i = \sigma_{ii} + \sigma_{ij} + \sigma_{ik} \quad (34)$$

where  $\sigma_{ii}$ ,  $\sigma_{ij}$  and  $\sigma_{ik}$  are the equilibrating stresses in the elastic spring, the Kelvin units and the shrinkage or swelling unit in  $i, j$ , and  $k$  directions, respectively. The equilibrating stress in each branch activates the total strain,  $\varepsilon_i$ , which constitutes of the elastic,  $\varepsilon_i^e$ , the viscoelastic,  $\varepsilon_i^{ve}$ , and the mechanosorptive,  $\varepsilon_i^{ms}$ , strains, and the strain due to shrinkage or swelling,  $\varepsilon_i^s$ ,

$$\varepsilon_i = \varepsilon_i^e + \varepsilon_i^{ve} + \varepsilon_i^{ms} + \varepsilon_i^s. \quad (35)$$

Similarly, the shear stress,  $\tau_{\alpha\beta}$ , activates the total shear strain,  $\gamma_{\alpha\beta}$ , which is the sum of the elastic shear strain,  $\gamma_{\alpha\beta}^e$ , the viscoelastic shear strain,  $\gamma_{\alpha\beta}^{ve}$ , and the mechanosorptive shear strain,  $\gamma_{\alpha\beta}^{ms}$ ,

$$\gamma_{\alpha\beta} = \gamma_{\alpha\beta}^e + \gamma_{\alpha\beta}^{ve} + \gamma_{\alpha\beta}^{ms}. \quad (36)$$

The constitutive equation of the linear elastic orthotropic material is written as

$$\begin{Bmatrix} \sigma_x \\ \sigma_y \\ \sigma_z \\ \tau_{yz} \\ \tau_{zx} \\ \tau_{xy} \end{Bmatrix} = \begin{bmatrix} Q_{xx}^e & Q_{xy}^e & Q_{xz}^e & 0 & 0 & 0 \\ Q_{yx}^e & Q_{yy}^e & Q_{yz}^e & 0 & 0 & 0 \\ Q_{zx}^e & Q_{zy}^e & Q_{zz}^e & 0 & 0 & 0 \\ 0 & 0 & 0 & Q_{yzs}^e & 0 & 0 \\ 0 & 0 & 0 & 0 & Q_{zxs}^e & 0 \\ 0 & 0 & 0 & 0 & 0 & Q_{xys}^e \end{bmatrix} \begin{Bmatrix} \varepsilon_x^e \\ \varepsilon_y^e \\ \varepsilon_z^e \\ \gamma_{yz}^e \\ \gamma_{zx}^e \\ \gamma_{xy}^e \end{Bmatrix} \quad (37)$$

or in a matrix notation

$$\boldsymbol{\sigma} = \mathbf{Q}^e \boldsymbol{\varepsilon}^e \quad (38)$$

where  $\mathbf{Q}^e$  is the elastic stiffness matrix,  $\boldsymbol{\sigma}$  is the stress vector and  $\boldsymbol{\varepsilon}^e$  is the elastic strain vector. Inverse of  $\mathbf{Q}^e$  is the elastic compliance matrix,  $\mathbf{J}^e = (\mathbf{Q}^e)^{-1}$ , expressed as

$$\mathbf{J}^e = \begin{bmatrix} 1/E_x & -\nu_{yx}/E_y & -\nu_{zx}/E_z & 0 & 0 & 0 \\ -\nu_{xy}/E_x & 1/E_y & -\nu_{zy}/E_z & 0 & 0 & 0 \\ -\nu_{xz}/E_x & -\nu_{yz}/E_y & 1/E_z & 0 & 0 & 0 \\ 0 & 0 & 0 & 1/G_{yz} & 0 & 0 \\ 0 & 0 & 0 & 0 & 1/G_{zx} & 0 \\ 0 & 0 & 0 & 0 & 0 & 1/G_{xy} \end{bmatrix}, \quad (39)$$

which is symmetric and consists of nine different nonzero components where  $\nu_{ij}$  are the Poisson's ratios,  $E_i$  the elastic moduli and  $G_{ij}$  the shear moduli for  $\{i, j\} = \{x, y, z\}$ . The viscoelastic constitutive equations are written as follows

$$\begin{Bmatrix} \sigma_x \\ \sigma_y \\ \sigma_z \\ \tau_{yz} \\ \tau_{zx} \\ \tau_{xy} \end{Bmatrix} = \begin{bmatrix} Q_{xx}^{ve} & Q_{xy}^{ve} & Q_{xz}^{ve} & 0 & 0 & 0 \\ Q_{yx}^{ve} & Q_{yy}^{ve} & Q_{yz}^{ve} & 0 & 0 & 0 \\ Q_{zx}^{ve} & Q_{zy}^{ve} & Q_{zz}^{ve} & 0 & 0 & 0 \\ 0 & 0 & 0 & Q_{yzs}^{ve} & 0 & 0 \\ 0 & 0 & 0 & 0 & Q_{zxs}^{ve} & 0 \\ 0 & 0 & 0 & 0 & 0 & Q_{xys}^{ve} \end{bmatrix} \begin{Bmatrix} \varepsilon_x^{ve} \\ \varepsilon_y^{ve} \\ \varepsilon_z^{ve} \\ \gamma_{yz}^{ve} \\ \gamma_{zx}^{ve} \\ \gamma_{xy}^{ve} \end{Bmatrix} + \begin{bmatrix} \eta_{xx}^{ve} & \eta_{xy}^{ve} & \eta_{xz}^{ve} & 0 & 0 & 0 \\ \eta_{yx}^{ve} & \eta_{yy}^{ve} & \eta_{yz}^{ve} & 0 & 0 & 0 \\ \eta_{zx}^{ve} & \eta_{zy}^{ve} & \eta_{zz}^{ve} & 0 & 0 & 0 \\ 0 & 0 & 0 & \eta_{yzs}^{ve} & 0 & 0 \\ 0 & 0 & 0 & 0 & \eta_{zxs}^{ve} & 0 \\ 0 & 0 & 0 & 0 & 0 & \eta_{xys}^{ve} \end{bmatrix} \begin{Bmatrix} \dot{\varepsilon}_x^{ve} \\ \dot{\varepsilon}_y^{ve} \\ \dot{\varepsilon}_z^{ve} \\ \dot{\gamma}_{yz}^{ve} \\ \dot{\gamma}_{zx}^{ve} \\ \dot{\gamma}_{xy}^{ve} \end{Bmatrix} \quad (40)$$

or in a matrix form

$$\boldsymbol{\sigma} = \mathbf{Q}^{ve} \boldsymbol{\varepsilon}^{ve} + \boldsymbol{\eta}^{ve} \dot{\boldsymbol{\varepsilon}}^{ve} \quad (41)$$

where the matrices  $\mathbf{Q}^{ve}$  and  $\boldsymbol{\eta}^{ve}$  are symmetric and consist of the viscoelastic material parameters.  $\boldsymbol{\varepsilon}^{ve}$  is the viscoelastic strain vector and  $\dot{\boldsymbol{\varepsilon}}^{ve}$  is its time derivative. The mechanosorptive constitutive equation takes the matrix form

$$\boldsymbol{\sigma} = \mathbf{Q}^{ms} \boldsymbol{\varepsilon}^{ms} + |\dot{u}|^{-1} \boldsymbol{\eta}^{ms} \dot{\boldsymbol{\varepsilon}}^{ms} \quad (42)$$

where  $\boldsymbol{\varepsilon}^{ms}$  is the mechanosorptive strain vector,  $\dot{\boldsymbol{\varepsilon}}^{ms}$  is its time derivative and  $|\dot{u}|^{-1}$  is the inverse of the absolute value of the time derivative of moisture content. The mechanosorptive material parameters compose the symmetric matrices  $\mathbf{Q}^{ms}$  and  $\boldsymbol{\eta}^{ms}$ , which are written in the unabridged notations as

$$\mathbf{Q}^{ms} = \begin{bmatrix} Q_{xx}^{ms} & Q_{xy}^{ms} & Q_{xz}^{ms} & 0 & 0 & 0 \\ Q_{yx}^{ms} & Q_{yy}^{ms} & Q_{yz}^{ms} & 0 & 0 & 0 \\ Q_{zx}^{ms} & Q_{zy}^{ms} & Q_{zz}^{ms} & 0 & 0 & 0 \\ 0 & 0 & 0 & Q_{yzs}^{ms} & 0 & 0 \\ 0 & 0 & 0 & 0 & Q_{zxs}^{ms} & 0 \\ 0 & 0 & 0 & 0 & 0 & Q_{xys}^{ms} \end{bmatrix}, \quad (43)$$

$$\boldsymbol{\eta}^{ms} = \begin{bmatrix} \eta_{xx}^{ms} & \eta_{xy}^{ms} & \eta_{xz}^{ms} & 0 & 0 & 0 \\ \eta_{yx}^{ms} & \eta_{yy}^{ms} & \eta_{yz}^{ms} & 0 & 0 & 0 \\ \eta_{zx}^{ms} & \eta_{zy}^{ms} & \eta_{zz}^{ms} & 0 & 0 & 0 \\ 0 & 0 & 0 & \eta_{yzs}^{ms} & 0 & 0 \\ 0 & 0 & 0 & 0 & \eta_{zxs}^{ms} & 0 \\ 0 & 0 & 0 & 0 & 0 & \eta_{xys}^{ms} \end{bmatrix}. \quad (44)$$

The strains due to shrinkage and swelling of the material are defined as

$$\varepsilon_i^s = \alpha_i (u - u_{ref}) \quad (45)$$

where  $\alpha_i$  is the shrinkage and swelling coefficient in the material direction  $i$  and  $u_{ref}$  the reference moisture content. The material parameters in Eqs. (37)-(45) are positive constants ( $> 0$ ).

### 3.2.5 Material parameters

The described rheological models include numerous material parameters. Experimental methods that would give the required material parameters directly do not exist. A handful of material parameters, for instance, the elastic and the shear moduli or the shrinkage and swelling coefficients, can be determined indirectly from experimentally measured loads and displacements. The others are usually determined by curve fitting procedures of the numerical models against the experimental results. Not surprisingly, the models normally capture the experimentally obtained material's behavior very well; however, validation of the models is shown rarely. A substantial variation of the material properties of a natural material like wood makes the validation of the rheological models fairly complicated. Although, there are all sorts of experimental data available in the literature, the need for the new ones is always present. Beside the heterogeneity of wood that requires a lot of testing, the development of new advanced experimental methods and equipment brings new possibilities for acquiring always better, more accurate and novel results. At the same time, rising computational power and software developments also open

new options for solving complex systems of equations and the models' calibrations. In this thesis, an attempt towards the development of a reliable general 3D model for describing the rheological behavior of wood in changing environmental conditions is made by formulating, applying and analyzing the new 3D mechanical model.

## 4 Results and discussion

The main focus of the thesis is the new mechanical model. The model is studied in detail and is applied on several cases for the first time. The corresponding equations are implemented and solved in a finite element software. Firstly, the capabilities of the model are analyzed for isothermal and isohume conditions. The time-dependent or viscoelastic behavior of small softwood specimens under a sustained uniaxial tensile load and a compressive deformation is numerically modelled based on the experimental results. The analyses are carried out in two dimensions. The viscoelastic material parameters required in the model are determined by the least-squares fitting procedure of the numerical against the experimental results. The obtained viscoelastic material parameters are used in the 3D analyses to study the influence of grain orientation on the time-dependent creep of a wood block under the sustained constant tensile load. A thorough mathematical consideration of the 3D mechanical model for isothermal and isohume conditions is also shown. Furthermore, changing moisture contents in wood are included in the formulation of the mechanical model. The multi-Fickian moisture transport model is implemented in the same finite element software as the new mechanical model to determine the spatial and temporal distributions of moisture contents over the analyzed domains. The obtained moisture content fields are taken as the input data for the mechanical model. The mechanosorptive material parameters are obtained by fitting of the numerical to the experimental results of oak cubes exposed to a sustained compressive load and changing  $RH$ . Moreover, the influence of the characteristic material parameters of the multi-Fickian and the mechanical models is examined on the mechanical response of glulam specimens during wetting and drying. In what follows, the main results obtained throughout the work of the thesis are presented. The results in detail with comprehensive discussions are given in the enclosed papers.

### 4.1 Viscoelastic material parameters

The viscoelastic material parameters are determined in creep of four different wood species, i.e., Douglas fir (*Pseudotsuga menziesii*), Norway spruce (*Picea abies*), Japanese cypress (*Chamaecyparis obtusa*), and European beech (*Fagus sylvatica* L.), and in relaxation of Scots Pine (*Pinus sylvestris* L.). The

viscoelastic assembly of the spring and the Kelvin unit in series in each material direction of the new mechanical model (named K model) is extended with adding the linear dashpot (KD model) or the Kelvin unit in series (KK model) in each material direction. In this way, the three variants of the mechanical model also referred as three viscoelastic models of different complexity are obtained, depending on a number of material parameters required in the particular model. The three 1D viscoelastic assemblies are illustrated in Figure 7a, b and c.

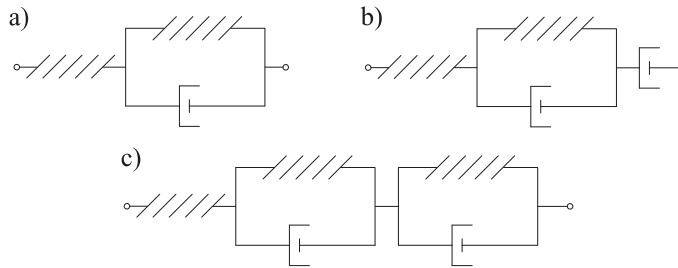


Figure 7. A schematic illustration of the rheological assemblies applied in the viscoelastic models, namely a) K, b) KD, and c) KK models.

In paper I, the three viscoelastic models are calibrated to the experimental results of time-dependent creep strains in the direction of applied constant tensile load and perpendicular to it (transverse). The viscoelastic material parameters in the longitudinal-transverse shear plane of Douglas fir (*Pseudotsuga menziesii*) wood species are determined for the three 1D viscoelastic models. A method presented in the European standard [91] and a method including relative errors are applied to evaluate numerically the accuracy of the particular model against the experimental results of creep strains in normal directions and shear. Both methods showed that all three viscoelastic models are suitable for predicting viscoelastic creep of wood. As expected, the comparisons show that the most complex model (KK) predicts the viscoelastic creep strains of wood in two material directions simultaneously better than the simplest (K) viscoelastic model. Nevertheless, the simplest model is estimated as good enough to predict the 2D viscoelastic creep of wood. As an example of the results of paper I, Figure 8 shows the viscoelastic strains in longitudinal,  $\varepsilon_L$ , and transverse,  $\varepsilon_T$ , directions of wood blocks of European beech (*Fagus sylvatica* L.) subjected to a constant tensile load in  $L$  direction. The viscoelastic strains in Figure 8 are shown as obtained experimentally [42] and predicted numerically with the three viscoelastic models.

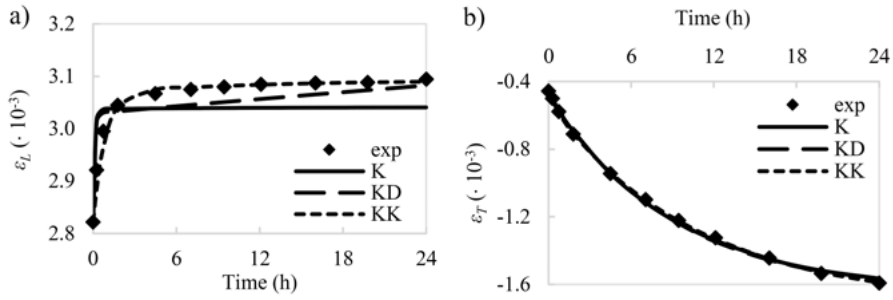


Figure 8. The viscoelastic creep strains in a) longitudinal and b) transverse directions of European beech (*Fagus sylvatica* L.) wood blocks exposed to a constant tensile load in longitudinal direction. The experimental data (exp) is extracted from [42] and predicted with three viscoelastic models (K, KD, and KK).

The ability of the three viscoelastic models to predict stress relaxation of wood is examined in paper II. Wood blocks of Scots pine (*Pinus sylvestris* L.) exposed to a stepwise constant deformation along and perpendicular to the grain are experimentally and numerically examined. The relaxation of stress and the viscoelastic strains along and perpendicular to the grain are determined. The experimental results of stress relaxation show a nonlinear viscoelastic behavior of wood over time. The nonlinearity gets more prominent under high deformation levels. The stress relaxation is higher in wood deformed along the grain than perpendicular to it. Figure 9 shows the stress-time curves obtained in the stress relaxation experiments and predicted with the three viscoelastic models along (L60) and perpendicular to the grain (T60), simultaneously. Each step during which the deformation is held constant and the stress relaxes takes 60 min. Similarly as for the viscoelastic creep, the most complex model (KK), including the highest number of viscoelastic material parameters, is the most successful in predicting the stress relaxation of wood under the stepwise deformation.

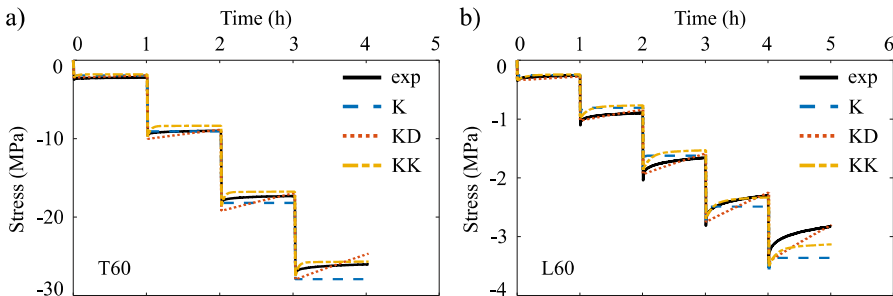


Figure 9. The stress-time curves of Scots Pine (*Pinus sylvestris* L.) blocks subjected to a stepwise deformation in a) longitudinal (L60) and b) transverse directions (T60) determined experimentally (exp) and predicted numerically by the viscoelastic models (K, KD, KK).

In paper III, the viscoelastic material parameters of Douglas fir (*Pseudotsuga menziesii*) wood species determined in paper I are applied in the 3D mechanical model (Eqs. (35)-(41)) to analyze the influence of grain orientation on the creep strains of a wood block under a sustained tensile load. In the numerical model, the orthotropic material directions in the analyzed specimen are assumed. The material directions are prescribed in the local coordinate system ( $t, l, r$ ). In the global Cartesian coordinate system ( $X, Y, Z$ ), the constant uniaxial tensile load,  $\sigma_Y$ , is applied and the total strains,  $\varepsilon_X, \varepsilon_Y, \varepsilon_Z$ , are observed over time. The rotation angles,  $\alpha_X$  and  $\alpha_Z$  about  $X$  and  $Z$  axes, respectively, simulate the misalignment of the material orthotropic directions relative to the directions of observations, i.e., the total strains in the global coordinate system. Figure 10 schematically illustrates a setup of the numerical model. It is assumed that the applied load induces the recoverable viscoelastic response of the material. The viscoelastic response is uniform over the entire geometry and strongly dependent on the prescribed viscoelastic parameters in the mechanical model. The focus of the performed numerical analyses is to observe the development of viscoelastic strains over time expressed in the global coordinate system at various inclinations of the material orthotropic directions. Thus, the strain and the stress magnitudes are of secondary importance and not studied here; however, the applied misalignments of the coordinate systems alter the strain magnitudes apparently.

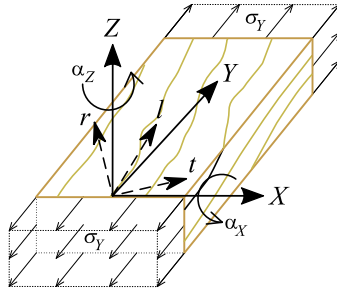


Figure 10. An illustration of the numerically analyzed wood specimen with the applied global ( $X, Y, Z$ ) and local ( $t, l, r$ ) coordinate systems, constant tensile load,  $\sigma_Y$ , and rotation angles  $\alpha_X$  and  $\alpha_Z$ .

The results of the numerical analyses in terms of the total strains,  $\varepsilon_X, \varepsilon_Y, \varepsilon_Z$ , are shown in Figure 11 for the applied rotation angles  $\{\alpha_X, \alpha_Z\} = \{0^\circ, 3^\circ, 6^\circ, 9^\circ\}$ . The elastic strains,  $\varepsilon_X^e, \varepsilon_Y^e, \varepsilon_Z^e$ , are suddenly activated at time 0. Their magnitudes are constant over time. At times  $> 0$ , the wood material creeps and the observed total strains,  $\varepsilon_X, \varepsilon_Y, \varepsilon_Z$ , are changing over time. When the material directions coincide with the global coordinate system where the load is prescribed and the total strains are observed, the numerical predictions of the material's behavior are presented by a solid line and marker  $\times$  in Figure 11. As expected, the material extends in longitudinal direction ( $Y$ ), which gives  $\varepsilon_Y > 0$ , and contracts in the transverse directions ( $X$  and  $Z$ ), i.e.,  $\varepsilon_X < 0$

and  $\varepsilon_Z < 0$ , over time under constant tension in longitudinal direction. Interestingly, when the rotations about  $Z$  axis,  $\alpha_Z = \{0^\circ, 3^\circ, 6^\circ, 9^\circ\}$ , at  $\alpha_X = 0^\circ$  are applied, the negative transverse strain  $\varepsilon_X$  increases over time (dashed lines in Figure 11a), which means that the wood specimen extends in  $X$  direction over time under constant tension in  $Y$  direction. Similarly, the rotations about  $X$  axis,  $\alpha_X = \{0^\circ, 3^\circ, 6^\circ, 9^\circ\}$ , at  $\alpha_Z = 0^\circ$  cause negative transverse strain  $\varepsilon_Z$  to increase over time (solid lines in Figure 11b). This kind of behavior could be interpreted as atypical or unnatural if the attention is not paid to the orientation of the material directions relative to the directions of observations. As shown in Figure 11c, the total strain  $\varepsilon_Y$  increases over time at any combination of the applied rotation angles  $\alpha_X$  and  $\alpha_Z$ .

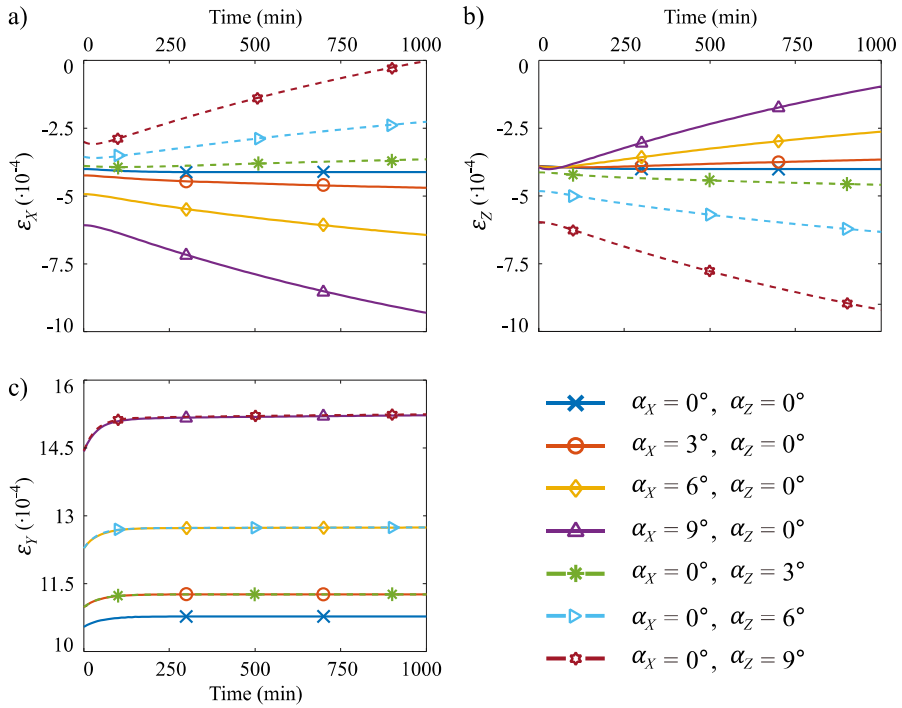


Figure 11. The time development of strains a)  $\varepsilon_X$ , b)  $\varepsilon_Z$ , and c)  $\varepsilon_Y$ , observed in the global coordinate system due to the sustained uniaxial load,  $\sigma_Y$ , for the applied rotation angles  $\alpha_X$  and  $\alpha_Z$  of the material coordinate system.

## 4.2 Mechanosorptive material parameters

In paper IV, the presented new mechanical model, including mechanosorption and shrinkage and swelling, is applied together with the multi-Fickian moisture transport model to determine moisture content fields. The performed 2D

numerical hygro-mechanical analysis is based on the available data and acquired results from testing of small cubes of European oak (*Quercus Robur* L.) exposed to constant uniaxial compression in  $T$  direction and changing  $RH$  of the ambient air. An illustration of the specimen's setup as implemented in the numerical model and the applied  $RH$  variation over time are shown in Figure 12a and b, respectively. The material parameters required in the moisture transport and the mechanical models are taken from the literature when possible. The unknown material parameters, such as the mechanosorptive and the viscoelastic material parameters, are obtained by the numerical fitting against the experimentally obtained total strains,  $\varepsilon_T$  and  $\varepsilon_R$ , which are determined as the average on the cube's surface. Figure 13 shows that the new mechanical model is able to predict the experimentally obtained total strains accurately in two orthotropic directions simultaneously. The corresponding viscoelastic and mechanosorptive material parameters determined in the framework of the presented hygro-mechanical analysis are suitable for future analyses of oak wood species exposed to mechanical loads and changing moisture contents.

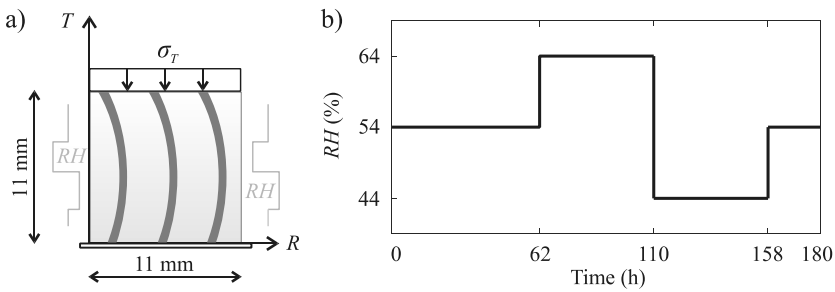


Figure 12. a) A schematic illustration of the specimen's setup as implemented in the numerical model; b) The applied  $RH$  variation over time.

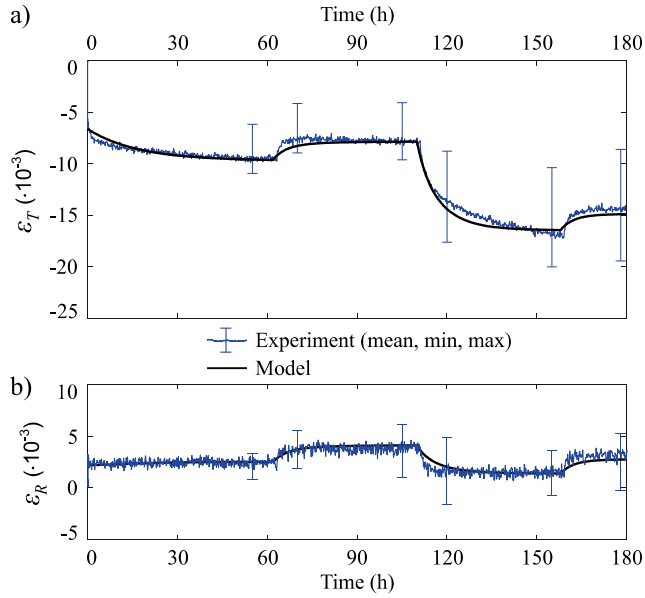


Figure 13. The total strains a)  $\varepsilon_T$  b)  $\varepsilon_R$  determined experimentally and predicted numerically in the analyzed specimen exposed to the sustained compressive stress,  $\sigma_T$ , and  $RH$  variation.

In paper V, the rheological behavior of wood exposed to  $RH$  changes in the absence of mechanical excitations is analyzed by means of the new mechanical model in combination with the multi-Fickian moisture transport model. The hygro-mechanical analysis is performed on glulam specimens of Norway spruce (*Picea abies*) exposed to  $RH$  changes from 50% to 90%  $RH$  (wetting) and from 90% to 50%  $RH$  (drying). The experimental data reported by Angst and Malo [92] are taken as a basis in the hygro-mechanical analysis. The moisture-induced strains and stresses in the analyzed glulam specimens are numerically determined in sections of equally thick slices. A schematic representation of the cross-sectional geometry with the notations of the global ( $XY$ ) and the local ( $rt$ ) coordinate systems, the slice numbers, and the edge exposed to the step changes of  $RH$  as considered in the numerical analysis is shown in Figure 14. The moisture transport analysis is applied in the global Cartesian coordinate system  $XY$ , while in the mechanical analysis, the cylindrical orthogonal coordinate system  $rt$  is applied to each lamella. The viscoelastic and the mechanosorptive material parameters required in the hygro-mechanical analyses are assumed on the experience from paper IV. The numerically predicted total,  $\varepsilon_X$ , and elastic,  $\varepsilon_X^e$ , strains in  $X$  (lengthwise) direction, as well as the moisture content of each slice,  $u$ , are compared to the experimental results [92] after 5, 12, 21 or 38 days of wetting and drying. The comparison shows that the hygro-mechanical model satisfactory captures the behavior of the glulam specimens exposed to wetting and drying.

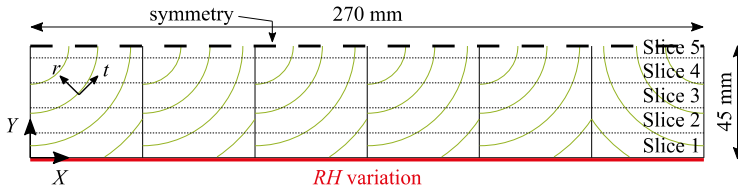


Figure 14. A schematic representation of the cross-sectional geometry with the notations of the global ( $XY$ ) and the local ( $rt$ ) coordinate systems, the symmetry line, the slices, the dimensions, and the edge exposed to  $RH$  changes from 50% to 90% (wetting) or from 90% to 50% (drying) considered in the numerical model.

Furthermore, the numerically predicted tensile stresses perpendicular to the grain in tangential direction,  $\sigma_t$ , are analyzed in the glulam specimens during wetting and drying. The analyses show that the moisture-induced maximum tensile stresses perpendicular to the grain are higher during drying ( $\sigma_t = 3.40$  MPa at 0.3 d) than wetting ( $\sigma_t = 0.63$  MPa at 0.3 d), which indicates that the analyzed specimen most probably cracks during drying due to the step change of  $RH$  from 90% to 50%. The tangential stresses,  $\sigma_t$ , predicted numerically after 0.3 d of drying from 90% to 50%  $RH$  and wetting from 50% to 90%  $RH$  are represented graphically on the deformed geometry of the glulam specimens in Figure 15c and Figure 16c, respectively. Figure 15a and b show the numerical predictions of  $u$  and  $\epsilon_X$ , respectively, in the glulam specimen after 0.3 d of wetting from 50% to 90%  $RH$ . Similarly, Figure 16a and b show the numerical predictions of  $u$  and  $\epsilon_X$ , respectively, in the glulam specimen after 0.3 d of drying from 90% to 50%  $RH$ .

To compare the moisture content, and the strain and the stress fields in the analyzed glulam specimens over time, Figure 17 and Figure 18 show numerical predictions of  $u$ ,  $\epsilon_X$  and  $\sigma_t$  after 5 d of wetting from 50% to 90%  $RH$  and drying from 90% to 50%  $RH$ , respectively. From comparisons of Figure 15 to Figure 17, it is seen that the moisture penetrates deeper in the glulam specimen over time, which (a) results in more significant changes of  $u$ ; (b) enlarges the total strains  $\epsilon_X$ ; (c) relaxes the tangential stresses  $\sigma_t$ ; and increases the deformations in general. Similarly, from comparisons of Figure 16 to Figure 18, it is seen that (a)  $u$  changes significantly in the glulam specimen, which, in general, causes (b) a decrease of  $\epsilon_X$ , (c) a relaxation of  $\sigma_t$ ; and an increase of deformations.

Additionally, in paper V, the influence of the characteristic material parameters required in the hygro-mechanical analyses on the mechanical behavior of the glulam specimens exposed to wetting and drying is studied extensively. Nevertheless, the studied material parameters required in the multi-Fickian moisture transport model and the mechanical model influence the mechanical behavior of glulam specimens exposed to the  $RH$  changes quite significantly, the overall mechanical behavior is still captured very well.

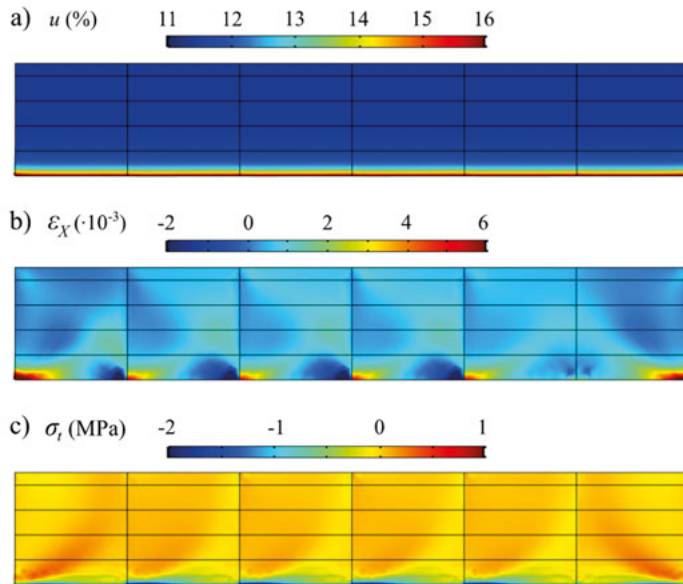


Figure 15. a) Moisture contents, b) total strains, and c) tangential stresses predicted numerically in the glulam specimen after 0.3 d of wetting from 50% to 90% RH. Graphical representations are shown on the deformed geometry with the magnification factor 5.

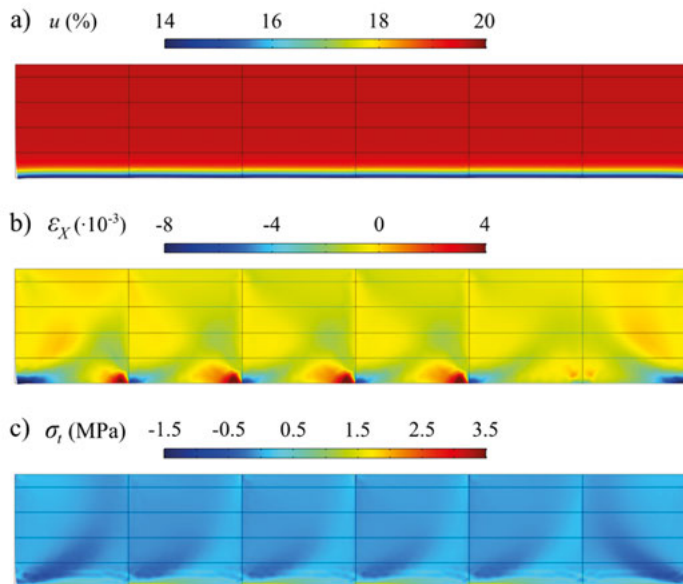


Figure 16. a) Moisture contents, b) total strains, and c) tangential stresses predicted numerically in the glulam specimen after 0.3 d of drying from 90% to 50% RH. Graphical representations are shown on the deformed geometry with the magnification factor 5.

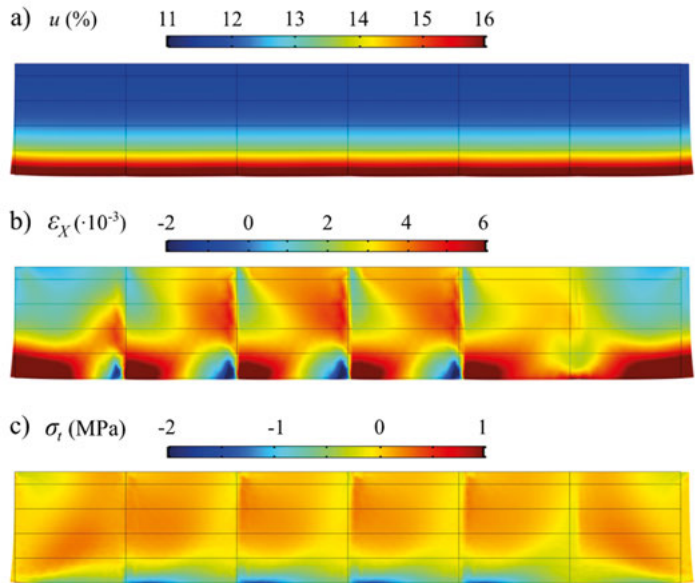


Figure 17. a) Moisture contents, b) total strains, and c) tangential stresses predicted numerically in the glulam specimen after 5 d of wetting from 50% to 90% RH. Graphical representations are shown on the deformed geometry with the magnification factor 5.

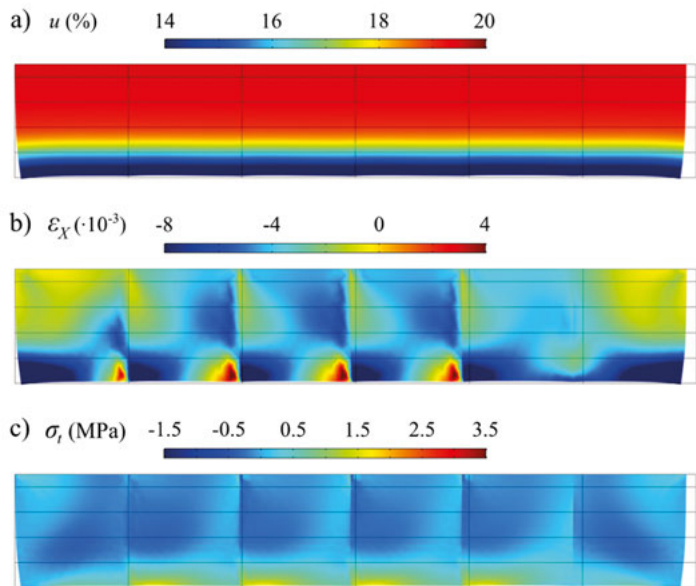


Figure 18. a) Moisture contents, b) total strains, and c) tangential stresses predicted numerically in the glulam specimen after 5 d of drying from 90% to 50% RH. Graphical representations are shown on the deformed geometry with the magnification factor 5.

## 5 Conclusions

In the present thesis, which main body are the enclosed papers, the rheological behavior of wood subjected to mechanical loads and deformations was examined in constant and changing climates. The aim of the thesis was to study numerically the long-term mechanical behavior of different wood species. For that purpose, the new 3D mechanical model was formulated and implemented in the finite element software. The new mechanical model was able to simulate the long-term response of the orthotropic material in all material directions simultaneously. The model additively included the elastic, the viscoelastic and the mechanosorptive responses, as well as the shrinkage and swelling. For describing the mechanosorptive response and the shrinkage and swelling, the mechanical model required the spatial and temporal distributions of moisture contents in wood due to changes in  $RH$  of the surrounding environment. The moisture content fields were determined by means of the advanced multi-Fickian moisture transport model, which was also implemented in the same finite element software.

The addressed mechanical model required a number of material parameters. While the elastic material parameters and the shrinkage and swelling coefficients have been well represented in the literature for various wood species, the viscoelastic and the mechanosorptive material parameters applicable for the used mechanical model did not exist initially. Therefore, three variants of the new mechanical model of different complexity, depending on a number of the viscoelastic material parameters required in the particular model, were applied to several sets of 2D experimental data of the viscoelastic creep of strain and the relaxation of stress. The analyses showed that already the simplest variant of the new mechanical model, with the lowest number of viscoelastic material parameters, was able to capture the viscoelastic creep behavior of wood specimens under compression very well. That was not the case for wood specimens under the stepwise deformation where only the most complex variant of the mechanical model, with the highest number of viscoelastic material parameters, was able to predict the viscoelastic behavior in stress relaxation. A significant influence of relatively small misalignments of the orthotropic directions relative to the directions of observed strains and applied sustained load on the viscoelastic response of a wood block was shown with the application of the mechanical model, including the obtained viscoelastic material parameters.

Furthermore, the non-uniform moisture content in wood was considered in the new mechanical model. The hygro-mechanical analyses, comprising of the moisture transport and the mechanical analyses, were applied to different cases. In the first case, the cubes of hardwood were exposed to the sustained compressive load and  $RH$  variations. The material parameters required in the models were determined partially by fitting of the numerical results to the experimental results, which turned out to be in a very good agreement. In the second case, the hygro-mechanical analysis was applied to the glulam specimens exposed to drying or wetting from one side. The required material parameters were adopted after the performed analysis in the first case. The numerically predicted moisture contents and strains agreed well with the reported experimental results in the literature. The performed parametric studies showed that the material parameters required in the multi-Fickian moisture transport model and the mechanical model influence the mechanical behavior of glulam specimens exposed to drying or wetting significantly. Nevertheless, the overall mechanical behavior of glulam specimens was still captured very well in general. Thus, the possibility of crack initiation in wood could be identified from the predicted magnitudes of the maximum tensile stresses perpendicular to the grain quite successfully.

The new mechanical model presented in the thesis showed great potential and suitability to predict the rheological behavior of softwoods and hardwoods when exposed to mechanical loads or deformations, acting in constant or varying  $RH$  conditions. The presented mechanical model in combination with the advanced multi-Fickian moisture transport model was able to estimate the long-term behavior of timber members exposed to  $RH$  changes also when the required material parameters were not known precisely. Nevertheless, the future work might focus on the determination of the required material parameters, including specific, extensive, multi-dimensional experimental analyses of various wood species, loading modes and  $RH$  regimes. The mechanosorptive behavior of wood in shear needs thorough experimental investigation and subsequent calibration of the corresponding mechanosorptive material parameters in the mechanical model. An extensive validation is needed in the future for the mechanical model's reliable use in timber engineering and timber industry. To broaden the application possibilities of the presented mechanical model, the implantation of the irrecoverable strains is required, as well as an upgrade, accounting for a redistribution of the stresses due to crack initiation and development.

# Acknowledgements

My thesis is a result of collaboration of many people and institutions. At this occasion, I would like to express my gratitude to those who contributed to its completion.

First, I deeply thank my supervisor, Professor Staffan Svensson for giving me the opportunity to carry out this thesis. Thank you for introducing this very interesting research topic to me, sharing your knowledge and ideas, your supervision, long discussions, and all the help and advice regarding our work. My moving to and living in Sweden has not always been easy. Thank you very much for making it a bit less puzzling, more active and tasteful.

The financial support by Gunnar Ivarson's Foundation (Gunnar Ivarsons Stiftelse för Hållbart Samhällsbyggande, GIS) made this thesis possible. I also express my sincere gratitude to Mr. Gunnar Ivarson himself for such a kind and generous gesture of financing research in the field of civil engineering.

The work presented in the thesis was carried out at the University of Borås that provided the workplace, laboratory facilities, and administrative and IT support, which is highly appreciated. I also thank the personnel of the Department of Resource Recovery and Building Technology at the University of Borås, in particular Johan, Madumita, Linda, Agnes, Kimmo and Lenart for their help during my stay in Borås and all the fun times we have had together.

I appreciate Uppsala University for accepting me as a doctoral student, offering the courses and publishing the thesis. I would especially like to thank Professor Kristofer Gamstedt at the Division of Applied Mechanics for all the bureaucratic effort, advice and assistance given regarding my studies at Uppsala University. The advice and help from the current and the former personnel of the Division of Applied Mechanics is also acknowledged.

I would also like to acknowledge the personnel of the Chair of Mechanics at the Faculty of Civil and Geodetic Engineering, University of Ljubljana, for hosting me as a visiting student and all the knowledge and help provided during my graduate studies.

I am most grateful to my family for standing by my side during my whole life. I also thank my friend Neja for the encouragement and support.

Finally, I sincerely thank my dearest Tomaž for always listening to my monologues so kindly and patiently. Thank you for believing in me at all those crazy moments and thank you for participating in pursuing my dreams. I could have never done it without you.

## Sammanfattning på svenska (Summary in Swedish)

För att konstruera säkra, tillförlitliga och beständiga träkonstruktioner för användning i naturliga utomhus- eller inomhusklimat krävs att trämaterialens fukt- och tidsberoende mekaniska beteende beaktas. Denna avhandling analyserar med, numerisk modellering och framtagna materialparametrar, träs fukt- och tidsberoende ur ett mekaniskt perspektiv. Den numeriska analysen är uppdelad i fukttransport och mekanisk analys. En kopplad Ficks fuktmodell används för att bestämma tids- och lägesberoende fukttillstånd, i det analyserade trämaterialiet, som resultat av att den omgivande luftens relativa fuktighet ( $RH$ ) varierar. Det beräknade fukttillståndet används som indata i den mekaniska analysen. Den mekaniska modellen, som här är framtagen, beräknar den reologiska responsen hos trämaterial i de tre ortotropa materialriktningarna. Modellen beräknar elastisk, viskoelastisk och mekanosorptiv respons, liksom krympning och svällning. Fukttransportmodellen och den mekaniska modellen är implementerade i ett numeriskt beräkningsprogram. Experimentellt bestämda materialparametrar från litteraturen används i de numeriska analyserna. Experimenten är utförda för olika träslag, med varierande deformation och belastning i konstanta eller varierande fuktförhållanden.

Den i detta arbete utvecklade mekaniska modellen kräver ett antal materialparametrar. De elastiska materialparametrarna och krympning-svällningskoefficienterna är väl representerade i litteraturen för olika träslag men det saknades inledningsvis, för modellen användbara, viskoelastiska och mekanosorptiva materialparametrar. I artikel I jämförs därför resultat från tre varianter av den nya mekaniska modellen med olika komplexitet, beroende på antalet materialparametrar, mot fyra uppsättningar data från krypförsök i konstant klimat. Analyserna visar att redan den enklaste varianten av den nya mekaniska modellen, med det lägsta antalet materialparametrar, klarar att förutse det tidsberoende beteendet hos tryckbelastade träprover mycket bra. I samma artikel bestäms de numeriska värdena för viskoelastiska materialparametrar för fyra träslag. I artikel II appliceras också de tre varianterna av den mekaniska modellen mot resultat från relaxationsförsök på träprover under stegvis ökande deformation. Analyserna visar att den mest komplexa varianten av den mekaniska modellen, med det högsta antalet materialparametrar, förutser det tidsberoende beteendet hos trä med tillfredställande noggrannhet.

I artikel III visas, genom mekanisk analys, hur känsliga krypmätningar är när det gäller materialriktningens orientering i förhållande till lastriktning. Även små avvikelser mellan träets ortotropa materialriktningar, i förhållande till de riktningar i vilka mätningar görs och last appliceras, påverkar de observerade mätresultaten signifikant. Denna kunskap är avgörande för att undvika feltolkning av försöksresultaten.

Vidare studeras transienta fuktillstånd i trä med den nya mekaniska modellen. Hygromekaniska studier, baserade på både fukttransport och mekaniska beräkningar, görs för motsvarande experimentella försök. I artikel IV exponeras provkuber av Ek (*Quercus robur*) för konstant trycklast och samtidig *RH*-variation. De materialparametrar som krävs i modellerna bestäms delvis genom att de numeriska resultaten kalibreras mot försöksresultaten. I artikel V jämförs den hygromekaniska modellen mot försöksresultat från limträprover som utsätts för ensidig uttorkning eller uppfuktning. Materialparametrarna antas från de tidigare utförda analyserna, och beräknade fuktinnehåll och töjningar överensstämmer väl med de rapporterade experimentella resultaten i litteraturen. Parameterstudierna visar att de materialparametrar som krävs av en kopplad Ficks fuktmodell och den mekaniska modellen påverkar det mekaniska beteendet hos limträprover som utsätts för uttorkning eller uppfuktning vid simulering. Det övergripande mekaniska beteendet hos limträprover är dock fortfarande fångat av modellen.

Den nya mekaniska modellen, som presenteras i avhandlingen, visar stor potential och lämplighet att förutsäga reologiskt beteende hos trämaterial vid exponering för mekaniska belastningar eller deformationer som verkar i konstanta eller varierande *RH*-förhållanden. Den presenterade mekaniska modellen i kombination med den kopplade Ficks fuktmodellen kan beräkna det tidsberoende beteendet hos träkonstruktioner som utsätts för varierande *RH*, även när de nödvändiga materialparametrarna inte är precist bestämda. Det framtida arbetet bör emellertid fokusera på bestämning av de nödvändiga materialparametrarna, genom erforderliga flerdimensionella experimentella analyser av olika träslag, belastnings- och klimatsituationer. En mer omfattande validering behövs i framtiden för den mekaniska modellens tillförlitlighet i olika tillämpningar inom träkonstruktioner och träindustri som inte beaktats i detta arbete.

## Povzetek v slovenščini (Summary in Slovenian)

V zadnjih letih se v razvitem svetu močno spodbuja raba obnovljivih virov in materialov, med katere spada tudi les kot naraven, obnovljiv in razgradljiv material. V gradbeništvu je raba lesa precej raznolika, od uporabe za nosilne sisteme stavb in inženirskih objektov, do uporabe za nenosilne konstrukcijske elemente, stavbno in notranje pohištvo, zunanje in notranje obloge tal, sten, stropov, ipd. Za doseg varne, učinkovite in vizualno privlačne uporabe lesa v konstrukcijske namene je ključno natančno razumevanje reološkega obnašanja lesa izpostavljenega mehanski obtežbi v spremenljivih pogojih okolja.

Doktorska disertacija, katere glavni del predstavljajo priloženi znanstveni članki, se posveča numeričnemu modeliranju dolgotrajnega mehanskega (reološkega) obnašanja lesa v pogojih konstantne in spreminjajoče se relativne vlažnosti zraka pri konstantni temperaturi. Les je obravnavan kot ortotropen material s tremi materialnimi smermi, in sicer longitudinalno smerjo vzdolž vlaken ter radialno in tangencialno smerjo, ki sta usmerjeni pravokotno na vlakna. Numerična analiza je zaporedno razdeljena na vlažnostno in mehansko analizo. V vlažnostni analizi je za določitev krajevnega in časovnega razporeda vsebnosti vlage v lesu, zaradi spreminjanja relativne vlažnosti zraka, uporabljen napredni, tako imenovani multi-Fickian vlažnostni model. Vsebnosti vlage se nato kot vhodni podatki uporabijo v mehanski analizi, kjer je za določitev reološkega obnašanja lesa uporabljen na novo razvit tridimenzionalni mehanski model. Ta temelji na predpostavki aditivnega razcepa skupne deformacije v posamezni materialni smeri na elastično, viskoelastično in mehanosorptivno deformacijo ter deformacijo zaradi krčenja ali nabrekanja lesa. Reševanje matematičnih enačb vlažnostnega in mehanskega modela se izvede s pomočjo komercialnega računalniškega programa, ki temelji na metodi končnih elementov. Mehanska analiza je izvedena na številnih primerih, ki obravnavajo različne vrste lesa, načine obremenitve in začetnega deformiranja konstrukcijskih elementov v pogojih konstantne in spreminjajoče relativne vlažnosti zraka. Izvedene numerične analize so podprte z eksperimentalnimi rezultati pridobljenimi iz literature ali iz samostojno izvedenih testov.

Uporabljen mehanski model vsebuje številne materialne parametre, pri čemer lahko nekatere najdemo v literaturi, kot na primer elastične in strižne

module ter koeficiente krčenja oziroma nabrekanja, medtem ko primerni viskoelastični in mehanosorptivni materialni parametri pred pričetkom raziskovalnega dela te doktorske disertacije niso bili poznani. Z namenom določitve viskoelastičnih materialnih parametrov in testiranja primernosti novega mehanskega modela za napovedovanje reološkega obnašanja lesa v konstantnih pogojih okolice so v prvem članku uporabljene tri različice novega mehanskega modela. Različice modela, ki se med seboj razlikujejo po številu vsebujočih viskoelastičnih materialnih parametrov, so uporabljene za napoved dvodimenzionalnega viskoelastičnega lezenja štirih vrst lesa. Opravljene numerične analize pokažejo, da je že najpreprostejši model oziroma njegova različica, ki vsebuje najmanjše število viskoelastičnih materialnih parametrov, primeren za napovedovanje viskoelastičnega lezenja lesa pod vplivom trajne enakomerne enoosne tlačne obremenitve. S primerjavo napovedi numeričnega modela in eksperimentalnih rezultatov pridobljenih iz literature so določene številčne vrednosti viskoelastičnih materialnih parametrov za analizirane vrste lesa. V drugem članku so enake tri različice mehanskega modela uporabljene za napovedovanje obnašanja lesenih vzorcev ene vrste iglavcev, ki so izpostavljeni odsekoma konstantni enoosni deformaciji. Primerjava numeričnih in lastnih eksperimentalnih rezultatov pokaže, da samo najkompleksnejša različica mehanskega modela, ki vsebuje največje število viskoelastičnih materialnih parametrov, zadovoljivo napove popuščanje oziroma relaksacijo napetosti in ravninsko deformiranje obravnavanih lesenih vzorcev.

Na podlagi viskoelastičnih materialnih parametrov, pridobljenih v prvem članku, je v tretjem članku izvedena tridimenzionalna numerična analiza vpliva orientacije materialnih smeri oziroma lesnih vlaken na reološko obnašanje lesa v konstantnih pogojih okolice. Izkazuje se, da imajo že relativno majhni zamiki materialnih smeri glede na smeri opazovanih deformacij in enakomerne natezne obremenitve relativno velik vpliv na opazovano viskoelastično obnašanje lesenega vzorca, kar je potrebno vzeti v obzir za pravilno interpretacijo eksperimentalnih rezultatov. V tretjem članku sta, poleg opisanih analiz, prikazana tudi matematična izpeljava uporabljenega mehanskega modela in dokaz simetrije viskoelastične podajnostne matrike.

V četrtem in petem članku sta na različnih primerih izvedeni vlažnostna in mehanska analiza, kjer sta uporabljena napredni vlažnostni model in nov mehanski model, ki vključuje tudi vpliv časovno in krajevno spreminjajoče se vsebnosti vlage v obravnavanih lesenih elementih. V četrtem članku je analizirano obnašanje hrastovega vzorca v obliki kocke pod vplivom enakomerne enoosne tlačne obremenitve in ciklično spreminjajoče relativne vlažnosti okoliškega zraka. S primerjavo numeričnih napovedi in eksperimentalnih rezultatov, ki se dobro ujemajo, so določeni viskoelastični in mehanosorptivni materialni parametri. Na podlagi teh in dodatnih materialnih parametrov, povzetih iz literature, so v petem članku izvedene numerične analize vzorcev iz lameliranega lepljenega lesa smreke, ki so

izpostavljeni dolgotrajnemu sušenju oziroma nabrekanju. Numerični rezultati vsebnosti vlage ter elastičnih in skupnih deformacij pri različnih časih se relativno dobro ujemajo z eksperimentalno pridobljenimi rezultati. Izvedene parametrične študije pokažejo precejšen vpliv nekaterih ključnih materialnih parametrov vlažnostnega in mehanskega modela na dobljene numerične rezultate. Kljub temu se lahko zadovoljivo oceni dolgotrajno mehansko obnašanje analiziranih vzorcev in napove možnost pojava razpok v smeri pravokotno na vlakna.

Izvedene analize in pridobljeni rezultati v tej doktorski disertaciji kažejo, da je predstavljen nov mehanski model zmožen in s tem primeren za napoved reološkega obnašanja lesa, izpostavljenega mehanski obtežbi pri spreminjajoči se relativni vlažnosti okoliškega zraka. Vendarle je za natančnejše numerične napovedi v prihodnje potrebno najprej, s pomočjo usmerjenih, večdimenzionalnih testov, določiti potrebne materialne parametre za različne vrste lesa ter obtežne in vlažnostne pogoje, nato pa na raznovrstnih primerih lesenih konstrukcijskih elementov in celotnih konstrukcij validirati mehanski model v kombinaciji z vlažnostnim modelom. Za razširitev uporabnosti in povečanje natančnosti mehanskega modela je priporočljiva tudi njegova nadgradnja z upoštevanjem materialne in geometrijske nelinearnosti ter razpok z redistribucijo napetosti.

# References

1. Larsen, K.E., Marstein, N. Conservation of Historic Timber Structures. An ecological approach. Oslo (2016).
2. Dinwoodie, J.M. Timber: Its nature and behavior. E & FN Spon, London and New York (2000).
3. Skaar, C. Wood-water relations, Springer Verlag, Berlin (1988).
4. Siau, J.F. Wood: Influence of moisture on physical properties. Department of Wood Science and Forest Products, Virginia Polytechnic Institute and State University, Keene (1995).
5. Zhang, X., Zilling, W., Künzel, H.M., Mitterer, C., Zhang, X. (2016) Combined effects of sorption hysteresis and its temperature dependency on wood materials and building enclosures – Part I: Measurements for model validation. *Building and Environment* 106:143-154.
6. Kollmann, F.F.P., Côté, W.A.Jr. Principles of Wood Science and Technology I, Solid Wood. Springer-Verlag, Berlin (1968).
7. Engelund, E.T., Thygesen, L.G., Svensson, S., Hill, C.A.S. (2013) A critical discussion of the physics of wood-water interactions. *Wood Science and Technology* 47(1):141-161.
8. Fortino, S., Mirianon, F., Toratti, T. (2009) A 3D moisture-stress FEM analysis for time dependent problems in timber structures. *Mechanics of Time-Dependent Materials*, 13(4):333-56.
9. Fragiaco, M., Fortino, S., Tononi, D., Usardi, I., Toratti, T. (2011) Moisture-induced stresses perpendicular to grain in cross-sections of timber members exposed to different climates. *Engineering Structures*, 33(11):3071-3078.
10. Reichel, S., Kaliske, M. (2015) Hygro-mechanically coupled modelling of creep in wooden structures, Part II: Influence of moisture content. *International Journal of Solids and Structures*, 77:45-64.
11. Angst, V., Malo, K.A. (2013) Moisture-induced stresses in glulam cross sections during wetting exposures. *Wood Science and Technology*, 47(2):227-241.
12. Ormarsson, S. Numerical Analysis of Moisture-Related Distortions in Sawn Timber. Chalmers University of Technology, Göteborg (1999).
13. Krabbenhöft, K., Damkilde, L. (2004) A model for non-Fickian moisture transfer in wood. *Materials and Structures*, 37(273):615-622.
14. Hanhijärvi, A. Modelling of creep deformation mechanisms in wood. Technical Research Centre of Finland, Espoo (1995).
15. Frandsen, H.L., Svensson, S., Damkilde, L. (2007) A hysteresis model suitable for numerical simulation of moisture content in wood. *Holzforschung*, 61(2):175-181.
16. Frandsen, H.L., Damkilde, L., Svensson, S. (2007) A revised multi-Fickian moisture transport model to describe non-Fickian effects in wood. *Holzforschung*, 61(5):563-572.
17. Frandsen, H.L., Svensson, S. (2007) Implementation of sorption hysteresis in multi-Fickian moisture transport. *Holzforschung*, 61(6):693-701.

18. Konopka, D., Kaliske, M. (2018) Transient multi-Fickian hygro-mechanical analysis of wood. *Computers & Structures*, 197:12-27.
19. Svensson, S., Turk, G., Hozjan, T. (2011) Predicting moisture state of timber members in a continuously varying climate. *Engineering Structures*, 33(11):3064-3070.
20. Hozjan, T., Svensson, S. (2011) Theoretical analysis of moisture transport in wood as an open porous hygroscopic material. *Holzforschung*, 65(1):97-102.
21. Schirmer, R. Die Diffusionszahl von Wasserdampf-Luftgemischen und die Verdampfungsgeschwindigkeit. VDI-Verl., Munich (1938).
22. Skaar, C., Siau, J.F. (1981) Thermal diffusion of bound water in wood. *Wood Science and Technology*, 15(2):105-112.
23. Hailwood, A.J., Horrobin, S. (1946) Absorption of water by polymers: Analysis in terms of a simple model. *Trans Faraday Soc*, 42:84-92.
24. Armstrong, L.D., Christensen, G.N. (1961) Influence of moisture changes on deformation of wood under stress. *Nature*, 191(479):869-870.
25. Armstrong, L.D., Kingston, R.S.T. (1960) Effect of moisture changes on creep in wood. *Nature*, 185(4716):862-863.
26. Schniewind, A.P. (1966) On Influence of Moisture Content Changes on Creep of Beech Wood Perpendicular to Grain Including Effects of Temperature and Temperature Changes. *Holz als Roh-und Werkstoff*, 24(3):87-98.
27. Grossman, P.U.A. (1976) Requirements for a model that exhibits mechano-sorptive behaviour. *Wood Science and Technology*, 10(3):163-168.
28. Fung, Y.C., Tong, P. Classical and computational solid mechanics. World Scientific Publishing Co. Pte. Ltd., Singapore (2001).
29. Findley, W.N., Lai, J.S., Onaran, K. Creep and relaxation of nonlinear viscoelastic materials. Dover, New York (1976).
30. Flügge, W. Viscoelasticity. Blaisdell Publishing Company, University of Michigan, Michigan (1967).
31. Tschoegl, N.W. The phenomenological theory of linear viscoelastic behavior: an introduction. Springer, Berlin (1989).
32. Schniewind, A.P., Barrett, J.D. (1972) Wood as a linear viscoelastic material. *Wood Science and Technology*, 6(1):43-57.
33. Hayashi, K., Felix, B., Le Govic, C. (1993) Wood viscoelastic compliance determination with special attention to measurement problems. *Materials and Structures*, 26(160):370-376.
34. Hunt, D.G., Shelton, C.F. (1987) Progress in the analysis of creep in wood during concurrent moisture changes. *Journal of Materials Science*, 22(1):313-320.
35. Hunt, D.G. (1986) The mechano-sorptive creep susceptibility of two softwoods and its relation to some other material properties. *Journal of Materials Science* 21(6):2088-2096.
36. Hering, S., Niemz, P. (2012) Moisture-dependent, viscoelastic creep of European beech wood in longitudinal direction. *European journal of wood and wood products*, 70(5):667-670.
37. Hunt, D.G. (1984) Creep trajectories for beech during moisture changes under load. *Journal of Materials Science*, 19(5):1456-1467.
38. Navi, P., Stanzl-Tschegg, S. (2009) Micromechanics of creep and relaxation of wood. A review COST Action E35 2004-2008: Wood machining – micromechanics and fracture. *Holzforschung* 63(2):186-195.
39. Halpin, J.C., Pagano, N.J. (1968) Observations on Linear Anisotropic Viscoelasticity. *Journal of Composite Materials*, 2(1):68-80.
40. Biot, M.A. (1954) Theory of Stress-Strain Relations in Anisotropic Viscoelasticity and Relaxation Phenomena. *Journal of Applied Physics*, 25(11):1385-1391.

41. Reichel, S., Kaliske, M. (2015) Hygro-mechanically coupled modelling of creep in wooden structures. Part I: Mechanics. *International Journal of Solids and Structures*, 77:28-44.
42. Özyhar, T., Hering, S., Niemz, P. (2013) Viscoelastic characterization of wood: Time dependence of the orthotropic compliance in tension and compression. *Journal of Rheology*, 57(2):699-717.
43. Kawahara, K., Ando, K., Taniguchi, Y. (2015) Time dependence of Poisson's effect in wood IV: influence of grain angle. *Journal of Wood Science*, 61(4):372-383.
44. Taniguchi, Y., Ando, K. (2010) Time dependence of Poisson's effect in wood I: the lateral strain behavior. *Journal of Wood Science*, 56(2):100-106.
45. Jiang, J., Valentine, B.E., Lu, J., Niemz, P. (2016) Time dependence of the orthotropic compression Young's moduli and Poisson's ratios of Chinese fir wood. *Holzforschung*, 70(11):1093-1101.
46. Ando, K., Mizutani, M., Taniguchi, Y., Yamamoto, H. (2013) Time dependence of Poisson's effect in wood III: asymmetry of three-dimensional viscoelastic compliance matrix of Japanese cypress. *Journal of Wood Science*, 59(4):290-298.
47. Hilton, H.H. (2001) Implications and constraints of time-independent Poisson ratios in linear isotropic and anisotropic viscoelasticity. *Journal of Elasticity*, 63(3):221-251.
48. Tschoegl, N.W., Knauss, W.G., Emri, I. (2002) Poisson's Ratio in Linear Viscoelasticity – A Critical Review. *Mechanics of Time-Dependent Materials*, 6(1):3-51.
49. Frandsen, H.L. Selected constitutive models for simulating the hygromechanical response of wood. Aalborg University, Denmark, pp 87–104 (2007).
50. Ranta-Maunus, A. (1975) Viscoelasticity of wood at varying moisture content. *Wood Science and Technology*, 9(3):189-205.
51. Lesse, P.F., Kingston, R.S.T. (1972) Osmotic Stress in Wood - Part II: Computation of Drying Stresses in Wood. *Wood Science and Technology*, 6(4):272-283.
52. Leicester, R.H. (1971) Rheological Model for Mechano-sorptive Deflections of Beams. *Wood Science and Technology*, 5(3):211-220.
53. Hanhijärvi, A. (2000) Advances in the knowledge of the influence of moisture changes on the long-term mechanical performance of timber structures. *Materials and Structures*, 33(225):43-49.
54. Ranta-Maunus, A. (1990) Impact of mechano-sorptive creep to the long-term strength of timber. *Holz als Roh- und Werkstoff*, 48(2):67-71.
55. Hunt, D.G. (1989) Linearity and non-linearity in mechano-sorptive creep of softwood in compression and bending. *Wood Science and Technology*, 23(4):323-333.
56. Toratti, T. Creep of timber beams in a variable environment. Technical Report no 31/TRT, Helsinki University of Technology (1992).
57. Salin, J.G. (1992) Numerical prediction of checking during timber drying and a new mechanosorptive creep model. *Holz als Roh- und Werkstoff*, 50(5):195-200.
58. Mårtensson, A., Svensson, S. (1997) Stress-strain relationship of drying wood. 1. Development of a constitutive model. *Holzforschung*, 51(5):472–478.
59. Mårtensson, A., Svensson, S. (1997) Stress-strain relationship of drying wood – Part 2: verification of a one-dimensional model and development of a two-dimensional model. *Holzforschung*, 51(6):565–570.
60. Svensson, S., Mårtensson, A. (2002) Simulation of drying stresses in wood. Part II. Convective air drying of sawn timber. *Holz als Roh- und Werkstoff*, 60(1):72-80.

61. Svensson, S., Toratti, T. (2002) Mechanical response of wood perpendicular to grain when subjected to changes of humidity. *Wood Science and Technology*, 36(2):145–156.
62. Dubois, F., Husson, J.M., Sauvat, N., Manfoumbi, N. (2012) Modeling of the viscoelastic mechano-sorptive behavior in wood. *Mechanics of Time-Dependent Materials*, 16(4):439-460.
63. Srpčič, S., Srpčič, J., Saje, M., Turk, G. (2009) Mechanical analysis of glulam beams exposed to changing humidity. *Wood Science and Technology*, 43(1-2):9-22.
64. Hunt, D.G., Shelton, C.F. (1987) Stable-state creep limit of softwood. *Journal of Materials Science Letters*, 6(3):353-354.
65. Hunt, D.G., Shelton, C.F. (1988) Longitudinal moisture-shrinkage coefficients of softwood at the mechano-sorptive creep limit. *Wood Science and Technology*, 22(3):199-210.
66. Hunt, D.G. (1989) Two classical theories combined to explain anomalies in wood behavior. *Journal of materials Science Letters*, 8(12):1474-1476.
67. Hunt, D.G., Gril, J. (1996) Evidence of physical ageing phenomenon in wood. *Journal of materials Science Letters*, 15(1):80-82.
68. Hunt, D.G. (2004) The prediction of long-time viscoelastic creep from short-time data. *Wood Science and Technology*, 38(7):479-492.
69. Husson, J.M., Dubois, F., Sauvat, N. (2010) Elastic response in wood under moisture content variations: analytic development. *Mechanics of Time-Dependent Materials*, 14(2): 203-217.
70. Dubois, F., Husson, J.M., Sauvat, N., Manfoumbi, N. (2012) Modeling of the viscoelastic mechano-sorptive behavior in wood. *Mechanics of Time-Dependent Materials*, 16(4):439-460.
71. Montero, C., Gril, J., Legeas, C., Hunt, D.G., Clair, B. (2012) Influence of hygro-mechanical history on the longitudinal mechanosorptive creep of wood. *Holzforschung*, 66(6):757-764.
72. Svensson, S. (1995) Strain and shrinkage force in wood under kiln drying conditions. 1. Measuring strain and shrinkage under controlled climate conditions - equipment and preliminary-results. *Holzforschung*, 49(4):363-368.
73. Svensson, S. (1996) Strain and shrinkage force in wood under kiln drying conditions. 2. Strain, shrinkage and stress measurements under controlled climate conditions. *Holzforschung*, 50(5):463-469.
74. Svensson, S., Martensson, A. (1999) Simulation of drying stresses in wood. Part 1: comparison between one- and two-dimensional models. *Holz als Roh- und Werkstoff*, 57(2):129-136.
75. Mårtensson, A. (1994) Mechano-sorptive effects in wooden material. *Wood Science and Technology*, 28(6):437-449.
76. Mohager, S., Toratti, T. (1993) Long term bending creep of wood in cyclic relative humidity. *Wood Science and Technology*, 27(1):49-59.
77. Gerhards, C.C. (1982) Effect of moisture content and temperature on the mechanical properties of wood. An analysis of immediate effects. *Wood and Fiber* 14(1):4-36.
78. Hanhijärvi, A., Mackenzie-Helnwein, P. (2003) Computational analysis of quality reduction during drying of lumber due to irrecoverable deformation. I: Orthotropic viscoelastic-mechanosorptive-plastic material model for the transverse plane of wood. *Journal of Engineering Mechanics-ASCE*, 129(9):996-1005.

79. Mackenzie-Helnwein, P., Hanhijärvi, A. (2003) Computational analysis of quality reduction during drying of lumber due to irrecoverable deformation. II: Algorithmic aspects and practical application. *Journal of Engineering Mechanics-ASCE*, 129(9):1006-1016.
80. Hassani, M.M., Wittel, F.K., Hering, S., Herrman, H.J. (2015) Rheological model for wood. *Computer Methods in Applied Mechanics and Engineering*, 283:1032-1060.
81. Hanhijärvi, A., Hunt, D. (1998) Experimental indication of interaction between viscoelastic and mechano-sorptive creep. *Wood Science and Technology*, 32(1):57-70.
82. Hanhijärvi, A. (1995) Deformation kinetics based rheological model for the time-dependent and moisture induced deformation of wood. *Wood Science and Technology*, 29(3):191-199.
83. Bažant, Z.P. (1985) Constitutive equation of wood at variable humidity and temperature. *Wood and Science Technology*, 19(2):159-177.
84. Englund, E.T, Svensson, S. (2011) Modelling time-dependent mechanical behaviour of softwood using deformation kinetics. *Holzforschung*, 65(2):231-237.
85. Eitelberger, J., Bader, T.K., de Borst, K., Jäger, A. (2012) Multiscale prediction of viscoelastic properties of softwood under constant climatic conditions. *Computational Materials Science*, 55:303-312.
86. Caulfield, D.F. (1985) A chemical kinetics approach to the duration-of-load problem in wood. *Wood and Fiber Science* 17(4):504-521.
87. Van der Put, T.A.C.M. Deformation and damage processes in wood. Delft University Press, Delft (1989).
88. Englund, E.T, Salmen, L. (2012) Tensile creep and recovery of Norway spruce influenced by temperature and moisture. *Holzforschung* 66(8):959-965.
89. Vidal-Salle, E., Chassagne, P. (2007) Constitutive equations for orthotropic nonlinear viscoelastic behaviour using a generalized Maxwell model. Application to wood material. *Mechanics of Time-Dependent Materials*, 11(2):127-142.
90. Krausz, A.S., Eyring, H. Deformation kinetics. John Wiley & Sons, New York (1975).
91. EN 1990 (2002) Annex D, Eurocode—Basis of structural design, Brussels.
92. Angst, V., Malo, K.A. (2012) The effect on climate variations on glulam—an experimental study. *European Journal of Wood and Wood Products*, 70(5):603-613.

# Acta Universitatis Upsaliensis

*Digital Comprehensive Summaries of Uppsala Dissertations  
from the Faculty of Science and Technology 1772*

Editor: The Dean of the Faculty of Science and Technology

A doctoral dissertation from the Faculty of Science and Technology, Uppsala University, is usually a summary of a number of papers. A few copies of the complete dissertation are kept at major Swedish research libraries, while the summary alone is distributed internationally through the series Digital Comprehensive Summaries of Uppsala Dissertations from the Faculty of Science and Technology. (Prior to January, 2005, the series was published under the title “Comprehensive Summaries of Uppsala Dissertations from the Faculty of Science and Technology”.)

Distribution: [publications.uu.se](http://publications.uu.se)  
urn:nbn:se:uu:diva-375148



ACTA  
UNIVERSITATIS  
UPSALIENSIS  
UPPSALA  
2019